CR-72930

10-047-009 (REV. 6/63)

DIVISION Power Sys. Div.

TM 4927:67-464

DATE 2 May 1967

W.O. 1041-01-0023

TECHNICAL MEMORANDUM

AUTHOR(S): F. P. Blissmer

TITLE: Structural Analysis and Evaluation of the 2nd Stage Nozzle Diaphragm - SNAP-8 Turbine Assembly

ABSTRACT

The magnitude and distribution of the elastic stresses and displacements in the SNAP-8 second stage turbine nozzle diaphragm (two-piece design) due to thermal and pressure loading conditions are determined.

Since the elastic stress level for the thermal transient condition exceeds the yield strength of the material (S-816), the structural integrity of the nozzle assembly is evaluated on the basis of low-cycle fatigue criteria.

An extremely conservative estimate of cyclic strain results in an expected life of 2700 cycles. More realistically though, it is shown that since the maximum elastic stress level is less than twice the yield strength, the stress-strain cycle will shake-down to elastic action after the first cycle of plastic deformation.

Based on maximum turbine performance requirements of 100 cycles, the 2nd stage nozzle diaphragm is structurally adequate to sustain the designated environmental loading conditions.

KEY WORDS

Nozzle Diaphragm, SNAP-8, Thermal Stress, Finite Element Method, Low-Cycle fatigue

APPROVED:
DEPARTMENT HEAD W. F. Banks

W. F. Banks

NOTE: The information in this document is subject to revision as analysis progresses and additional data are acquired.

STRUCTURAL ANALYSIS AND EVALUATION

OF THE 2nd STAGE NOZZLE DIAPHRAGM

SNAP-8 TURBINE ASSEMBLY

APRIL 1, 1967

Approved by:

H. D. Tabakman

H. D. Tabakman, Task Engineer
Turbine Task Force
Power Systems Division

H. Efron

H. E. Efron, Head
Stress Section, 4927
Power Systems Division

Prepared by:

F. P. Blissmer

F. P. Blissmer, Engineer
Turbine Task Force
Stress Section, 4927
Power Systems Division

STRUCTURAL ANALYSIS AND EVALUATION

OF THE 2nd STAGE NOZZLE DIAPHRAGM

SNAP-8 TURBINE ASSEMBLY

APRIL 1, 1967

Approved by:

H. D. Tabakman, Task Engineer
Turbine Task Force
Power Systems Division

H. E. Efron, Head
Stress Section, 4927
Power Systems Division

Prepared by:

F.P. Blissmer

F. P. Blissmer, Engineer
Turbine Task Force
Stress Section, 4927
Power Systems Division

TABLE OF CONTENTS

LIST OF FIGURES

I. INTRODUCTION

The magnitude and distribution of the stresses in the second stage turbine diaphragm and shroud are presented in this report. These stresses were obtained by using the finite element method of analysis.

Essentially, the method consists of idealizing an elastic body as a series of discreet elements interconnected at nodal points. The stiffness of each element is defined by its geometry and material properties; loads (mechanical and/or thermal) specified at the nodal points are used in solving the equilibrium equations. A general treatment of finite element techniques and applications is contained in Reference (1). Specifically, the theory and associated digital computer programs used in this report are explained in detail in References (2) and (3).

The analyses are in accord with the diaphragm-shroud component configuration shown in AGC Drawings 1264196-1 and 1264198-1. The general configuration and details of the "floating" vanes are shown in Figures 1 through 4.

The following loading cases, acting separately, were considered:

1. Thermal loading as indicated in Figures 8 through 11
2. Normal pressure of 75 psi.

One quadrant (with appropriate boundary conditions) of the diaphragm and shroud was considered. This is admissible since for all practical purposes double symmetry exists both in regard to geometry and distribution of thermal and mechanical loading.

II SUMMARY OF RESULTS

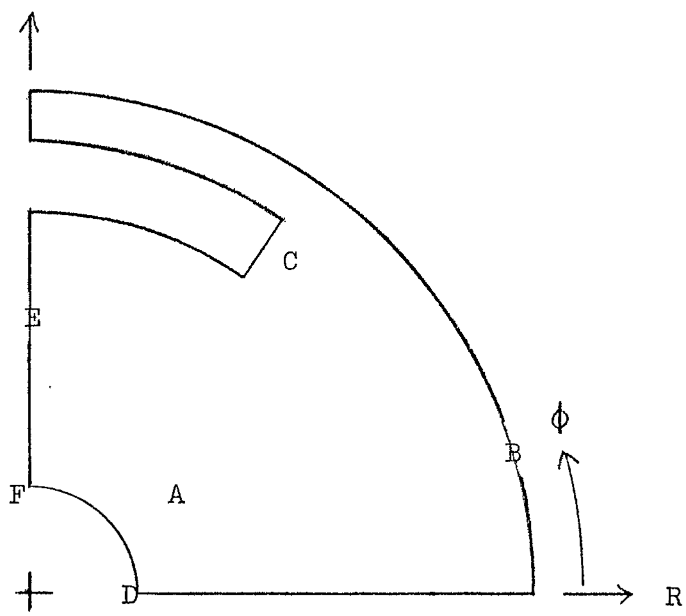

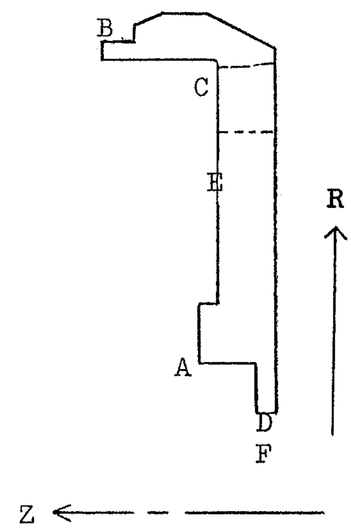

LOADING CONDITION		Maximum Stress (ksi)	Location on Sketch Above	Reference Page in Report	Maximum Displacement (inches)	Reference Page in Report	Location on Sketch Above
LOADING CONDITION	Case 1 - Thermal - Bending + In-Plane (Figs. 9, 10, 11)	Hub -30.0	A	43	Hub ΔZ = +0.0135	42	F
		Shroud +50	B	43	Shroud ΔR = +0.016	44	B
		Diaphragm -46	C	41			
	Case 2 - Normal Pressure = 75 psi	Hub +6.0	D	47	Hub ΔZ = -0.005	46	F
		Shroud -4.0	B	47			
		Diaphragm -10.0	E	45			

Maximum elastic stresses (50,000 psi) occur in the 2nd stage nozzle diaphragm at 16 seconds after turbine start-up due mainly to the large thermal gradients through the thickness of the diaphragm. The subsequent maximum stress level of 10,000 psi due to the pressure difference of 75 psi across the diaphragm is essentially constant during the remainder of an operational cycle (until turbine shut-down).

As shown in Appendix A, an extremely conservative estimate of cyclic strain shows an expected life of 2700 cycles. More realistically though, the maximum elastic stress level due to the thermal gradient at 16 seconds can be considered as a thermal shock occurring in an operational cycle of several hundred hours. Since the maximum elastic stress level is less than twice the yield strength, the stress-strain cycle will shake-down to elastic action (no further repeated plastic flow) fter the first cycle.

Based on maximum turbine performance requirements of 100 cycles (one cycle = start-up and shut-down operation), the 2nd stage nozzle diaphragm is structurally adequate to sustain the designated environmental loading conditions.

III. METHOD OF ANALYSIS

For both load cases (thermal and pressure) the analysis consists of determining the stresses in the diaphragm portion of the component by calculating equivalent structural members (elements) to represent the mechanical and thermal characteristics of the shroud and the hub. Although the effects of the shroud and hub on the diaphragm stresses can be represented quite accurately, the resulting stresses in these equivalent elements themselves are not sufficient. Thus stresses in the shround and hub components are determined by considering an axisymmetric (rotationally symmetric) cross-section.

A. THERMAL LOADING

The time at which the maximum stresses will occur was determined from a study of the temperature differences through the thickness of the diaphragm as a function of time. As can be seen from Figure 7, the maximum temperature differences and thus the maximum stresses, will occur at 16 seconds.

The stress distribution due to the radial, circumferential, and axial temperature gradients is composed of two parts:

1. In-plane stresses which are caused by movements of adjacent elements parallel to a median plane (mid-thickness).

2. Thermal bending stresses which are caused by a temperature difference through the thickness of an element.

The in-plane stresses are obtained from a generalized plane-stress finite element computer program using the temperature at mid-thickness (Figure 10) as the thermal loading.

The lateral bending stresses are obtained from a finite element computer program for plate bending using the thermal moment, M_T (see page 30) caused by the temperature difference through the thickness of each element (Figure 9).

1. Plane Stress Analysis

To account for the in-plane effects of the shroud, an equivalent ring forming an integral part of the diaphragm was substituted for the shroud.

This equivalence was based on the following:

a. The width of the ring measured in the radial direction equals that of the shroud in plan view.

b. The radial displacement of the ring when subject to an axisymmetric radial load equals that of the shroud when subject to the same loading. This condition leads to the establishment of the thickness of the ring as shown on page 26.

c. The radial displacement of the ring at its juncture with the diaphragm equals that of the shroud at the same location with the shroud subject to the thermal distribution remote from the window as shown in Figure 11. This condition leads to an equivalent coefficient of linear expansion for the ring with the latter subject to a uniform temperature as shown on page 26.

d. The region of the shroud bridging the cut-out (window) in the diaphragm is considered to be effectively 0.50 inches thick subject to a uniform temperature of 645°F. as shown in Figure 11(c). This is because the lower flange of the actual shroud is rendered ineffective due to the close pitch of a series of slots to hold the vanes in position (see Figure 3).

A detailed grid with numbered elements and nodal points is presented in Figure 6. The following boundary conditions were employed at the proper boundary nodal points as shown on page 22:

a. Along the edges of symmetry, the tangential displacements and shears vanish.

b. Along all free edges, the normal and shear stresses vanish.

To account for the variation in thickness of the elements shown in Figure 5, an equivalent modulus was used. As indicated in Table I, the equivalent modulus is defined as the product of the actual modulus of elasticity pertinent to a particular temperature and a corresponding actual thickness. It should be observed that the variation with temperature of the modulus of elasticity and coefficient of linear expansion were taken into account. These variations are presented in Figure 13, page 23.

2. Bending Analysis

Since the plate bending computer program does account for changes in thickness of the elements, the thickness of each element is input directly into the program.

The equivalent shroud ring for the bending case is based on the following:

a. The width of the ring measured in the radial direction equals that of the shroud in plane view.

b. The moment of inertia (about the center line of the diaphragm) of the ring is the same as that of the actual shroud cross-section. The calculations for the equivalent thickness of the ring with and without the vane cut-outs is shown on page 33.

c. Thermal moment on the shroud ring is input as zero. That this is the actual condition is evidenced by the thermal displacement pattern of the shroud shown in Figure 14. The rotation along the inner radius of the shroud ring where the diaphragm and the shroud are integral is essentially zero. The nodal point and element grid is the same as that used in the plane stress analysis (Figure 6).

The following boundary conditions were applied:

a. Along the edges of symmetry the normal shears, tangential rotations, and twisting moments vanish.

b. Along all other boundaries, the normal and twisting moments, and the normal shear vanish.

c. Nodal point 13 is used as a reference for displacements by setting the normal displacement, w, equal to zero.

3. Axisymmetric Analysis

To obtain the stress distribution in the shroud and hub, an axisymmetric finite element solution was employed on a cross-section where the shroud and diaphragm form an integral part as shown in Figure 18. It should be noted that in this representation, each element is actually a ring, and the geometry and loading have rotational symmetry. The temperature difference through the diaphragm is taken to be $300^{\circ}F$, and the temperatures in the hub and shroud are shown in Figure 25.

B. PRESSURE LOADING

The normal pressure loading (case 2) solution was obtained by two separate analyses.

1. Diaphragm stresses were calculated by using the plate bending program with the same finite element grid (Figure 6) and the same equivalent shroud as shown on page 33.

For the pressure analysis, the following boundary conditions were applied:

a. Along the edges of symmetry, the normal shears, tangential rotations, and twisting moments vanish.

b. Along the outer radius of the shroud at nodal points where ears are located (see page 35) the normal and twisting moments vanish, and the normal displacement is zero (simple support conditions).

c. Along the nodal points defining the window boundary, the normal load transferred to the diaphragm and shroud by the inserted vanes is input as a shear load as shown on pages 36 and 37.

d. Along the inner radius and other non-loaded free edges, the normal and twisting moments, and the normal shear vanish.

2. Hub and shroud stresses were obtained from an axisymmetric solution using the finite element grid shown in Figure 18. Pressure loading of 75 psi was applied and nodal point 169 was fixed in the axial direction as a displacement reference.

C. DISCUSSION OF RESULTS

1. Thermal Loading

Maximum principle stresses for both the thermal in-plane and thermal bending conditions are plotted in contour form in Figures 21 and 22 respectively. Based on the large bending stresses, the critical region is delineated as section A-A in Figure 23, and the individual components of the stresses are superimposed with respect to compression on the upstream face to obtain the maximum principle stress in the diaphragm of 46 ksi (compression).

From the axisymmetric solution the maximum thermal stresses in the shroud and hub regions are 50 ksi (tension) and 30 ksi (compression) respectively as shown in Figure 25.

Maximum normal displacement, .0135 inches in the upstream direction, occurs at the inner radius (hub) as shown in Figure 24b.

Maximum radial displacement of the shroud due to the net effect of radial growth and rotation is 0.016 inches as shown in Figure 26.

2. Pressure Loading

Maximum principle stresses for the bending condition produced by the pressure loading are plotted in contour form in Figure 27. It should be noted that the stresses indicated will be compression on the upstream face and tension on the downstream face. Maximum stress of 10.0 ksi occurs in the diaphragm below the window area.

From the results of the axisymmetric pressure solution presented in Figure 29, the maximum shroud and hub stresses are 4 ksi (compression) and 6.0 ksi (tension) respectively.

Normal displacements are shown in Figure 28, and the maximum, .005 inches in the downstream direction, occurs below the window at the inner radius (hub).

01-071-002

QUADRILLE WORK SHEET

AEROJET-GENERAL CORPORATION
AZUSA, CALIFORNIA

PAGE 10 OF ___ PAGES
DATE 20 MAR 1967
SUBJECT 2ND STAGE NOZZLE DIAPHRAGM BY S. AXTENS WORK ORDER 7310·23·100
SNAP·8

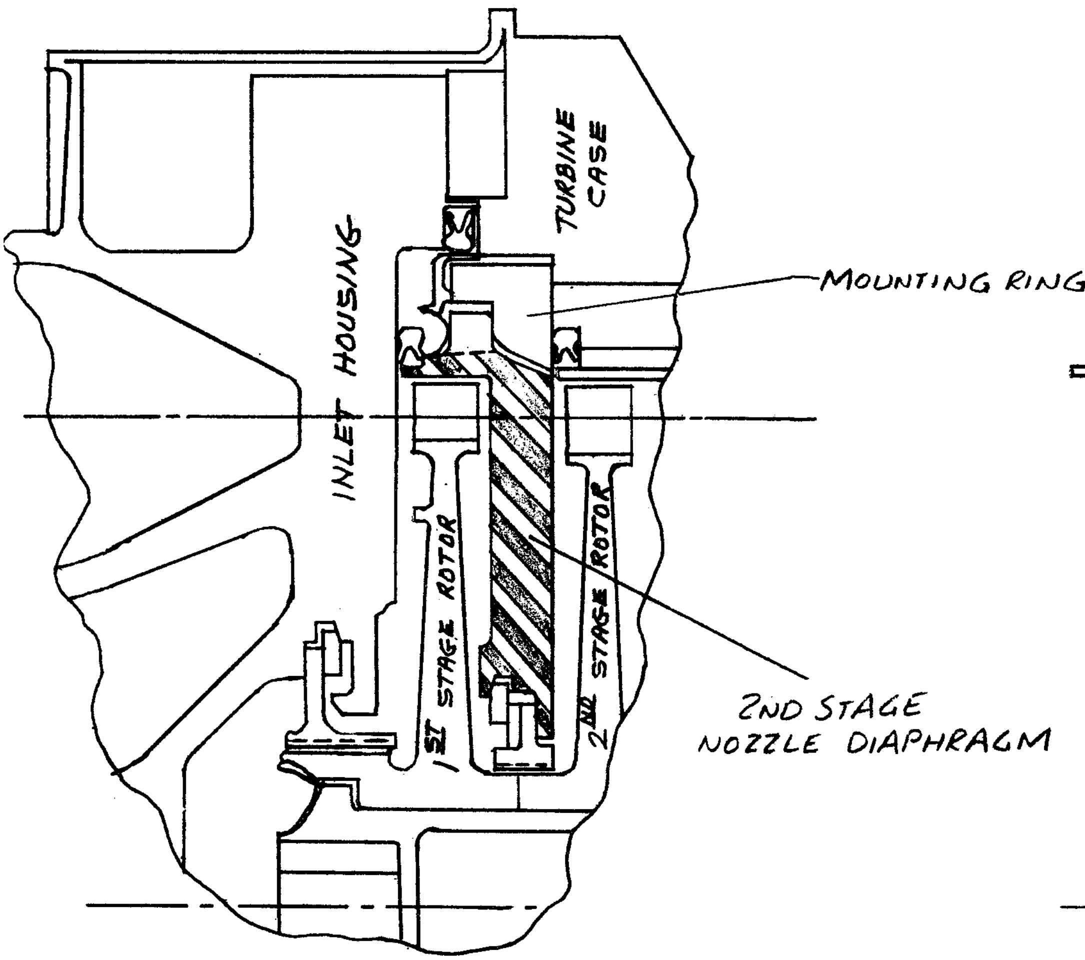

a.) LAYOUT

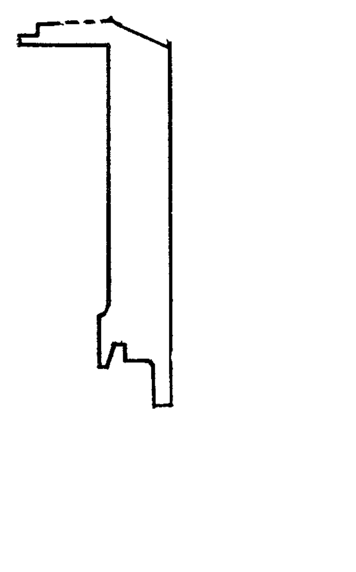

b.) FREE-BODY DIAGRAM

LAYOUT CONFIGURATION AND FREE-BODY SKETCH OF SECOND-STAGE NOZZLE DIAPHRAGM

FIG. 1

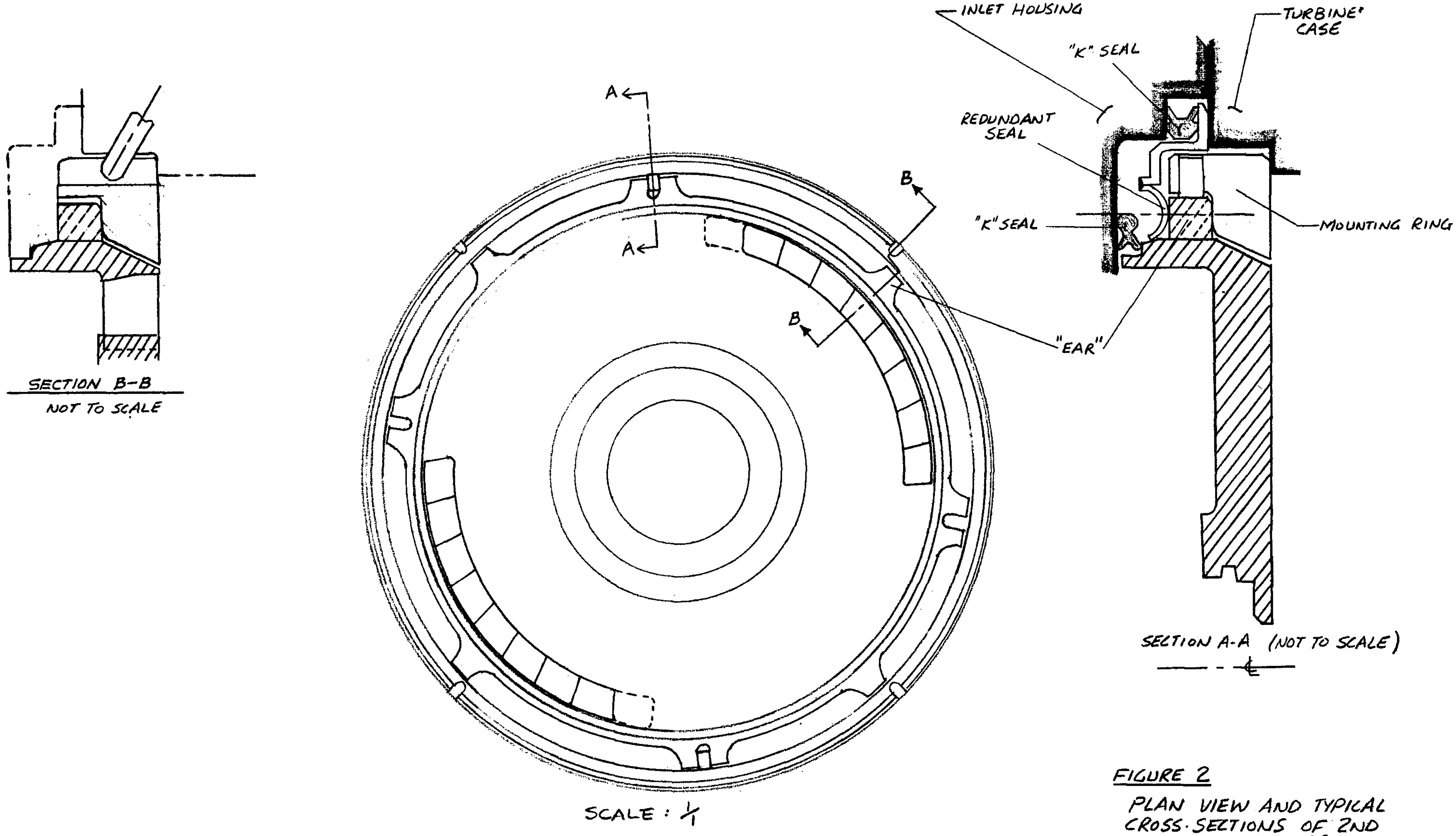

FIGURE 2

PLAN VIEW AND TYPICAL CROSS-SECTIONS OF 2ND STAGE NOZZLE DIAPHRAGM ASSEMBLY

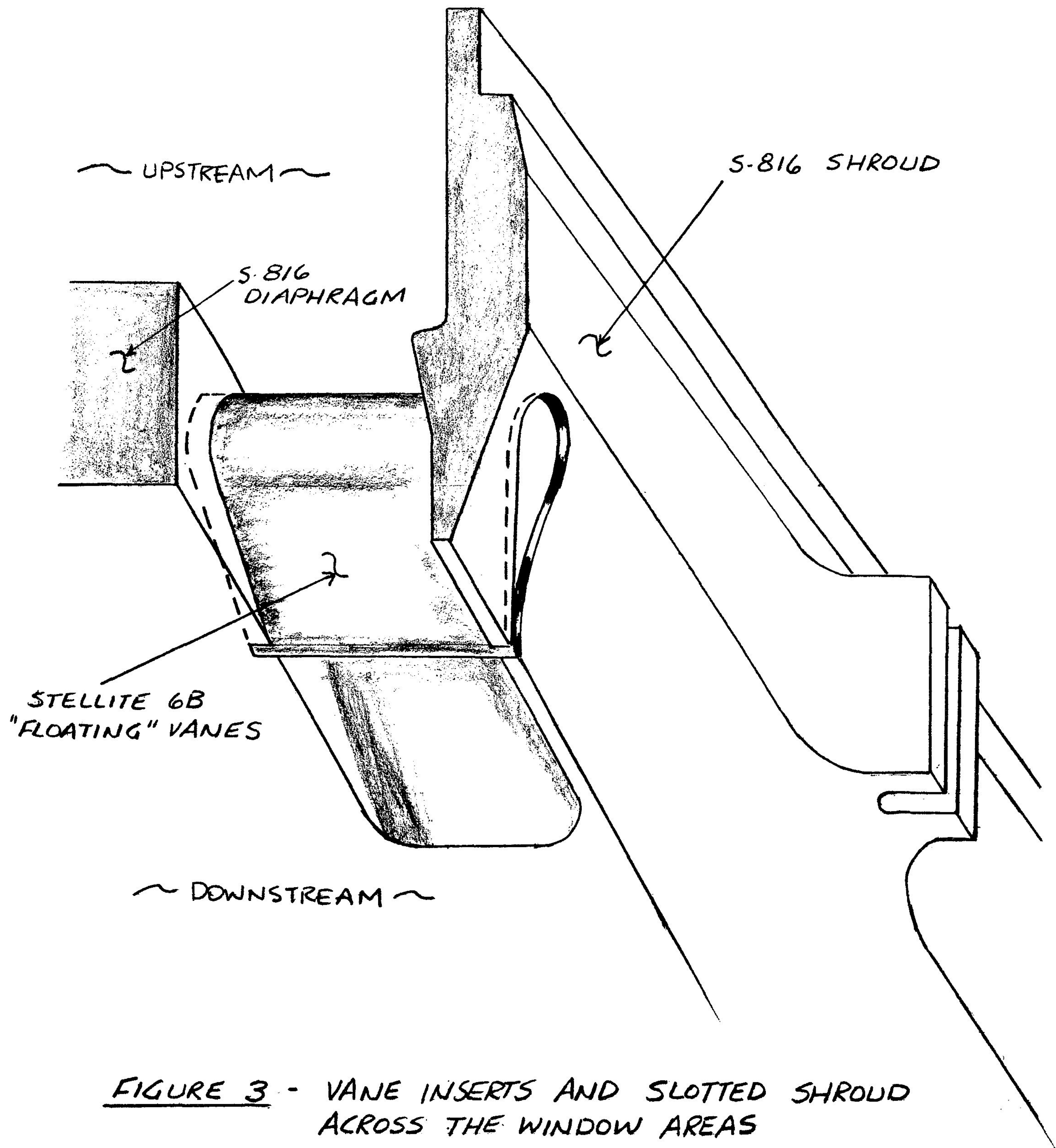

FIGURE 3 - VANE INSERTS AND SLOTTED SHROUD ACROSS THE WINDOW AREAS

01-071-002

QUADRILLE WORK SHEET

AEROJET-GENERAL CORPORATION
AZUSA, CALIFORNIA

PAGE 13 OF ____ PAGES
DATE 17 MAR 1967
SUBJECT 2ND STAGE NOZZLE DIAPHRAGM BY FPB WORK ORDER 7310·23·100
SNAP·8

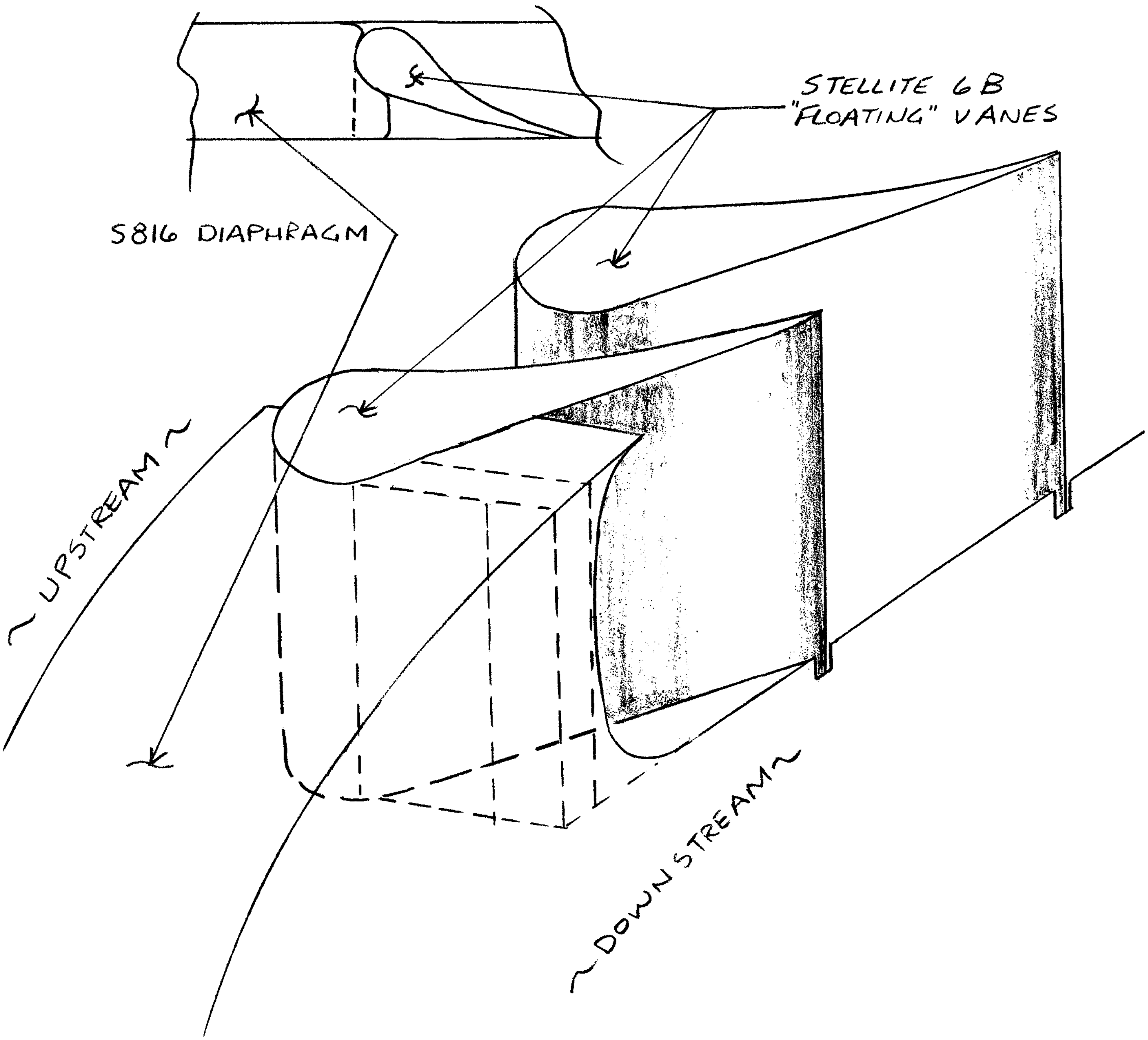

FIGURE 4 - END WALL VANE INSERT SKETCH WITH SHROUD REMOVED

567-NF-1107

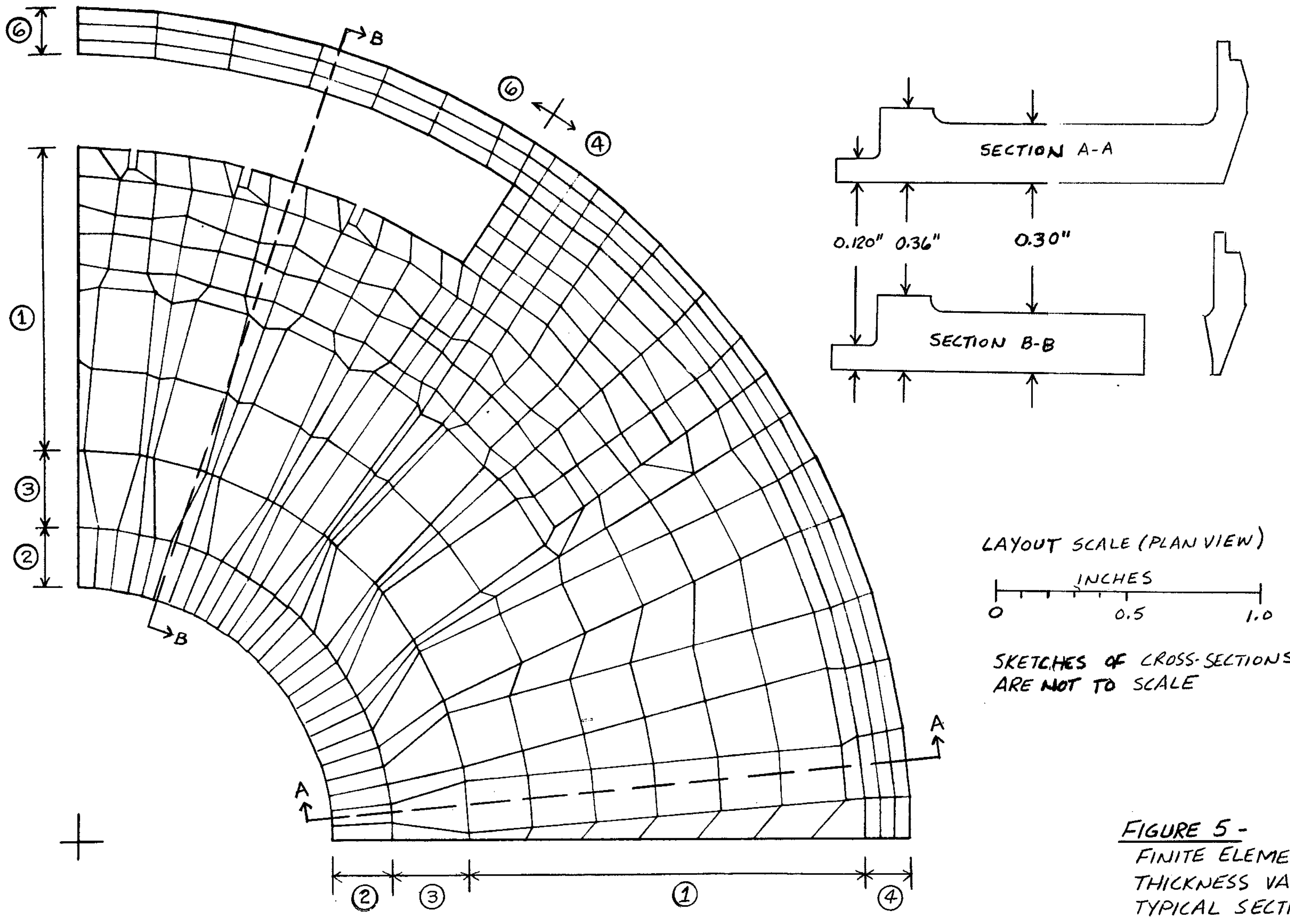

LEGEND

(n) REFERS TO MATERIAL NUMBER [SEE PAGE 24]

FIGURE 5 -
FINITE ELEMENT GRID SHOWING THICKNESS VARIATIONS THROUGH TYPICAL SECTIONS

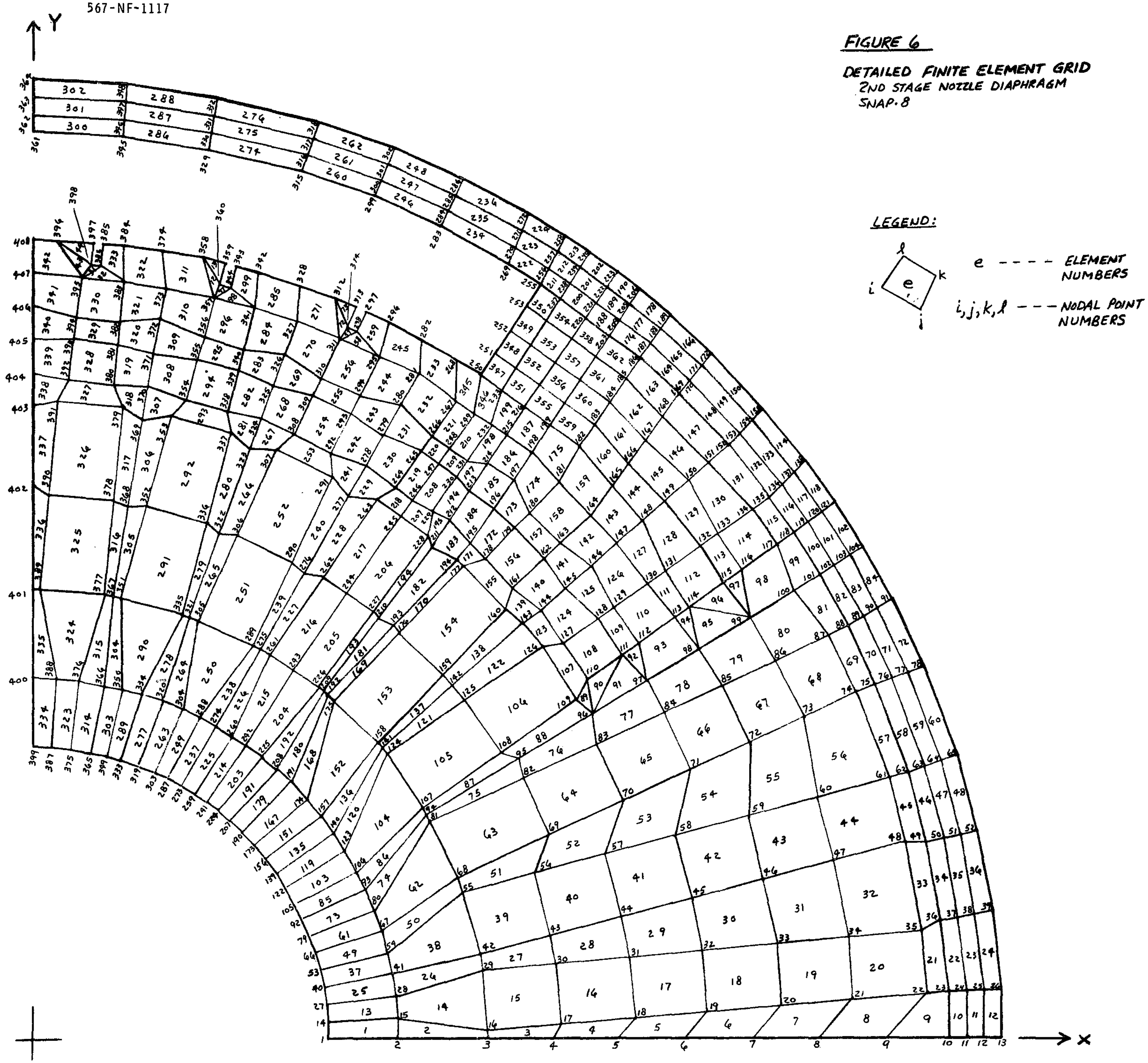

FIGURE 6

DETAILED FINITE ELEMENT GRID
2ND STAGE NOZZLE DIAPHRAGM
SNAP-8

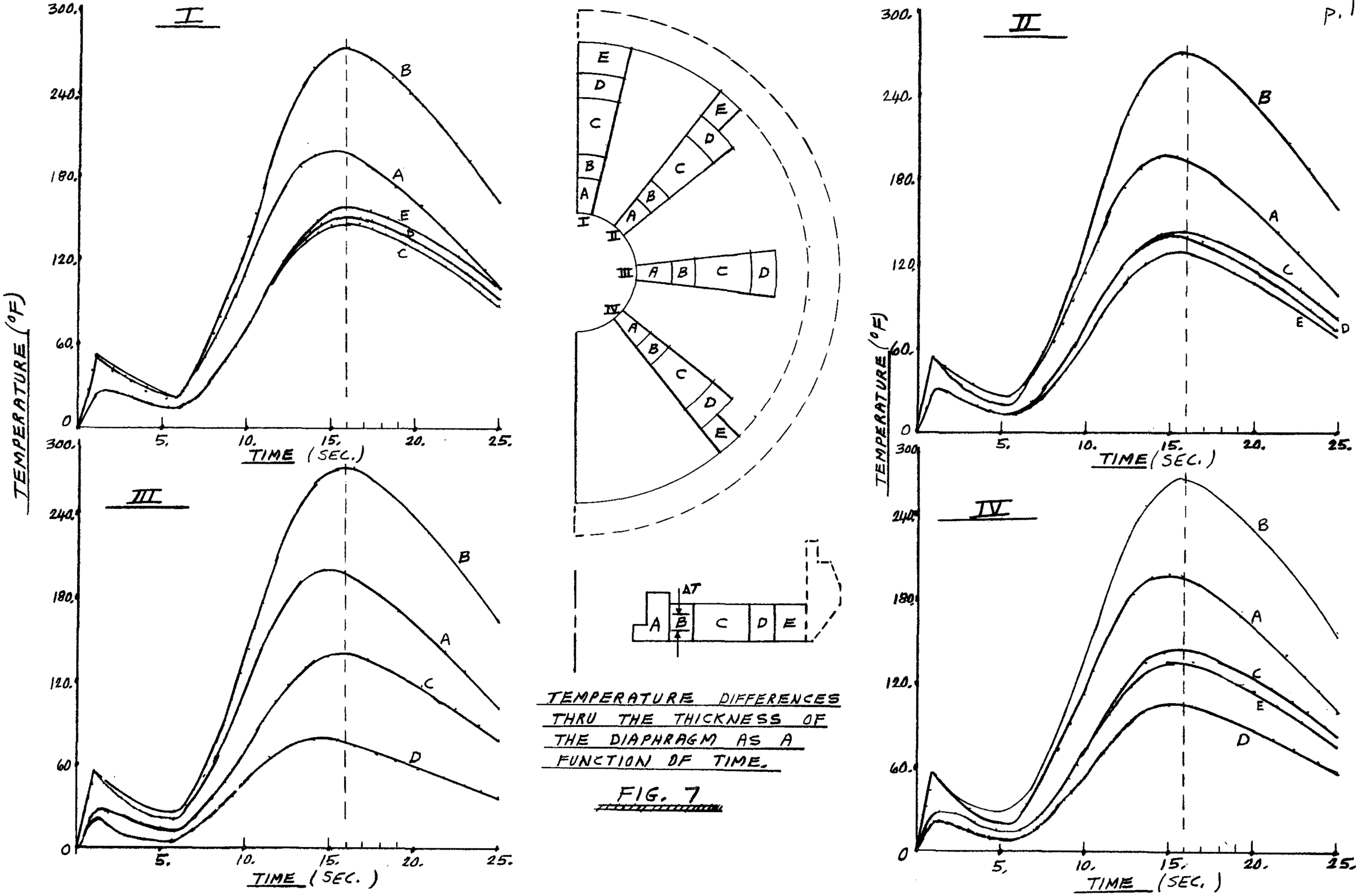

TEMPERATURE DIFFERENCES THRU THE THICKNESS OF THE DIAPHRAGM AS A FUNCTION OF TIME.

FIG. 7

01-071-002

QUADRILLE WORK SHEET

AEROJET-GENERAL CORPORATION
AZUSA, CALIFORNIA

PAGE 17 OF ____ PAGES

DATE 3 MAR 1967

SUBJECT 2ND STAGE NOZZLE DIAPHRAGM BY FPB WORK ORDER 7310.23-100
SNAP-8

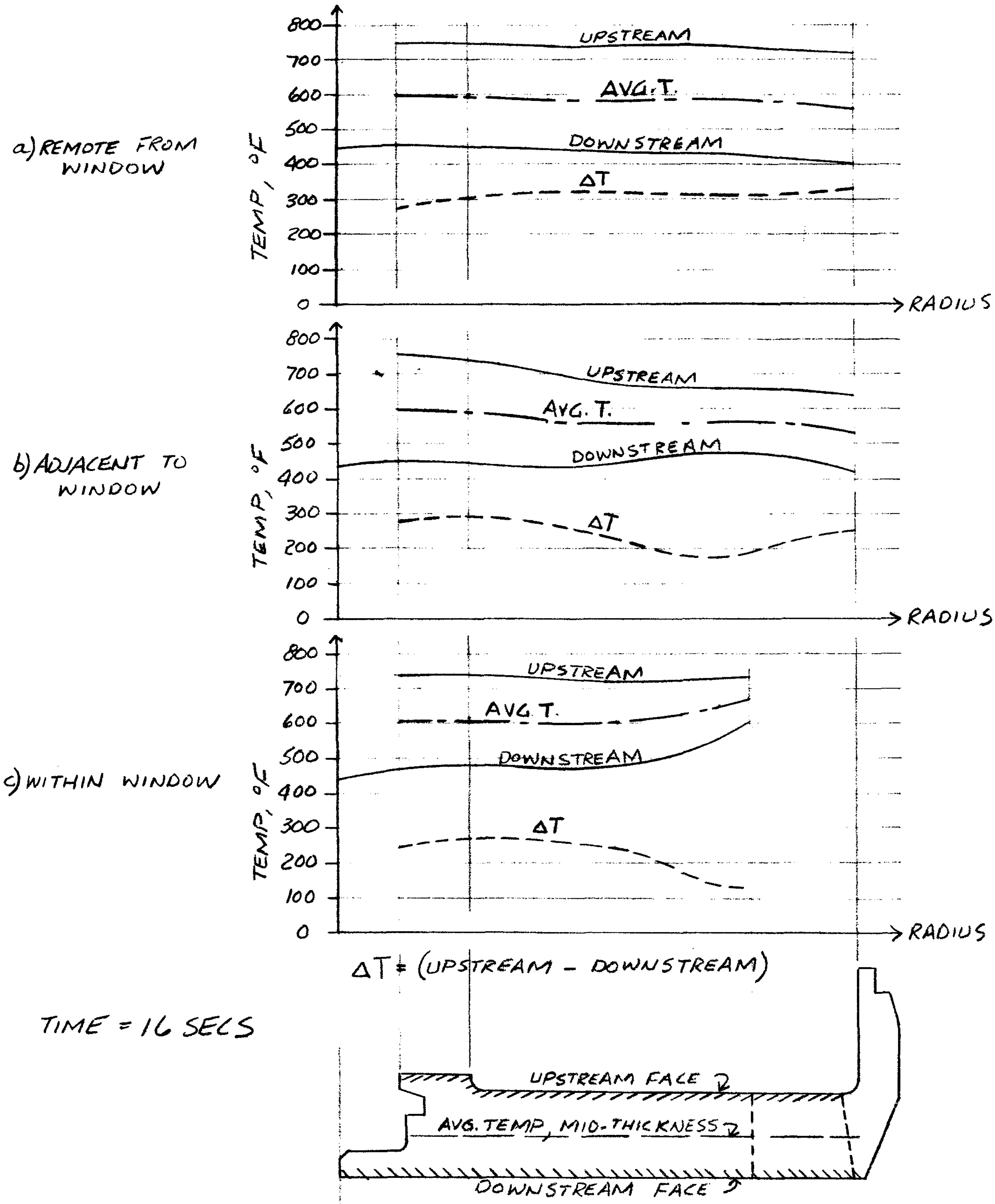

FIGURE 8 - TEMPERATURE IN DIAPHRAGM CROSS-SECTIONS

FIGURE 9
THERMAL MAP - TEMPERATURE DIFFERENCES OF UPSTREAM AND DOWNSTREAM FACES

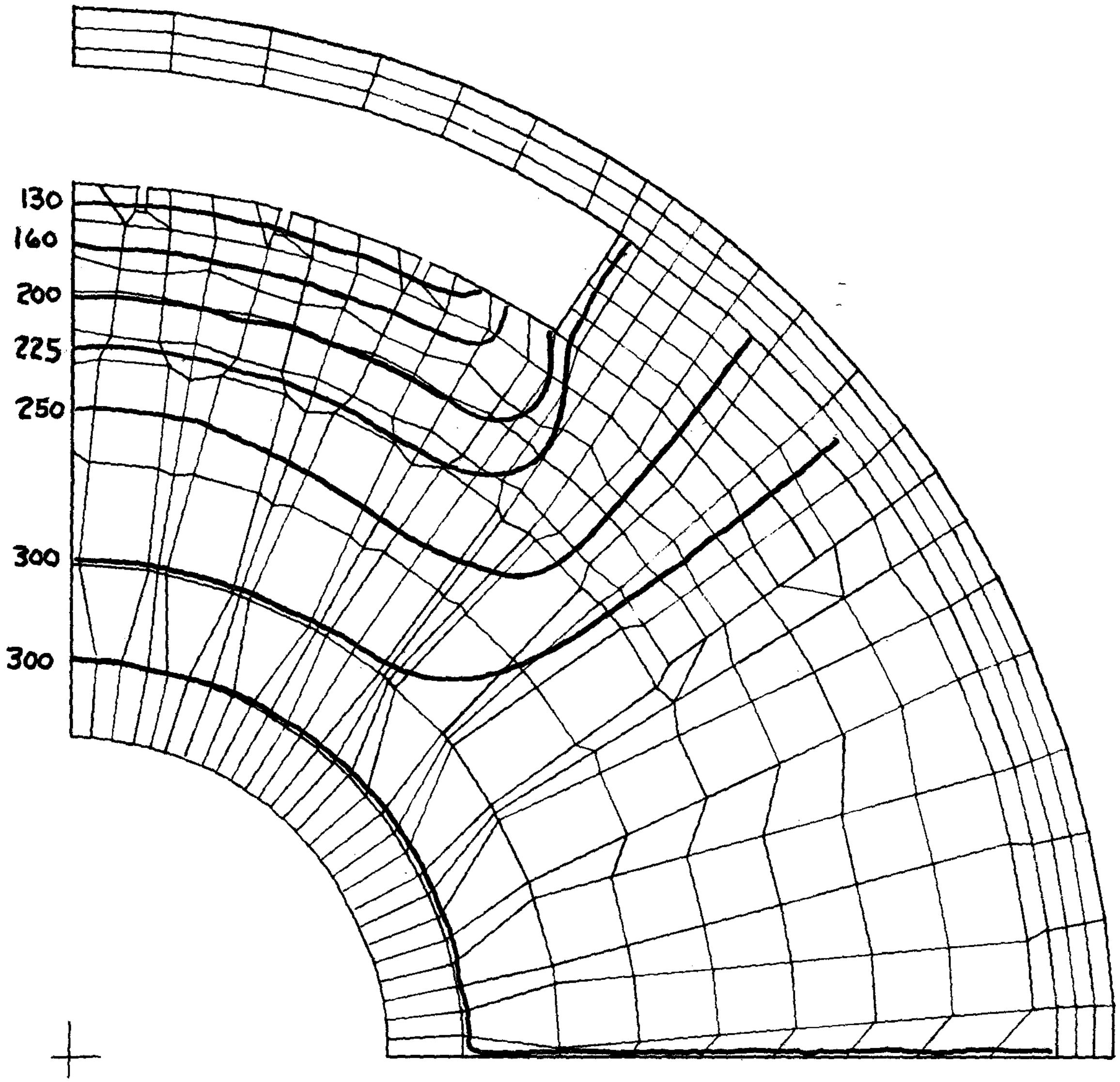

TEMPERATURE DIFFERENCE (ΔT) CONTOURS, °F

ΔT = UPSTREAM FACE TEMPERATURE
− DOWNSTREAM FACE TEMPERATURE

FIGURE 10
THERMAL MAP - IN-PLANE TEMPERATURE DISTRIBUTION ON DIAPHRAGM

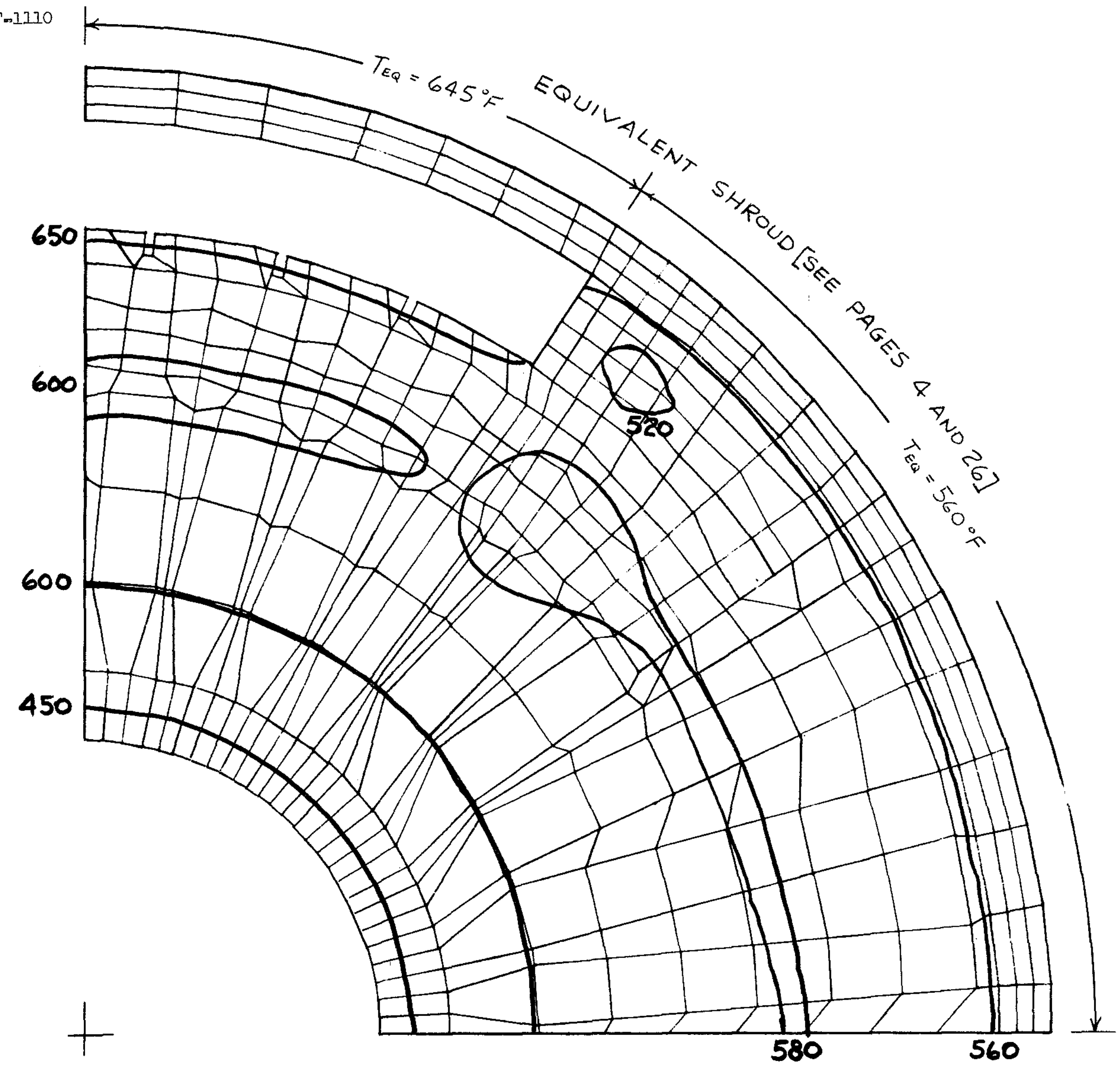

TEMPERATURE CONTOURS, °F
AT MID-THICKNESS OF DIAPHRAGM

01-071-002

QUADRILLE WORK SHEET

AEROJET-GENERAL CORPORATION
AZUSA, CALIFORNIA

PAGE 20 OF ____ PAGES
DATE 14 MAR 1967
WORK ORDER 7310·23·100
SNAP·8

SUBJECT 2ND STAGE NOZZLE DIAPHRAGM BY FPB

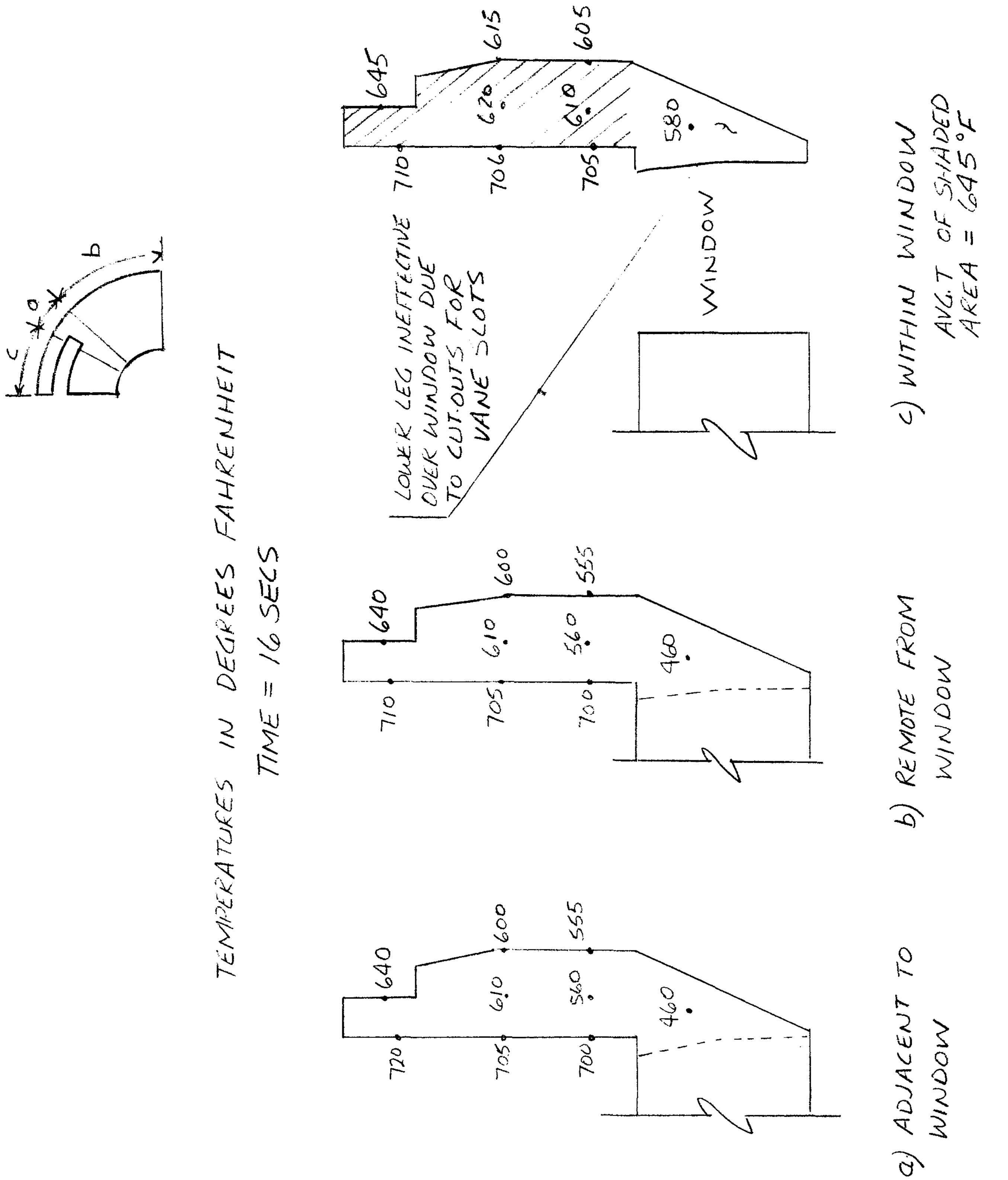

FIGURE 11 - TEMPERATURE DISTRIBUTION IN SHROUD CROSS-SECTIONS

IV ANALYSIS AND CALCULATIONS

BASIC ASSUMPTIONS

1. GEOMETRY AND TEMPERATURE DISTRIBUTION ARE SYMMETRICAL ABOUT TWO AXES (DOUBLE SYMMETRY) AS SHOWN BELOW:

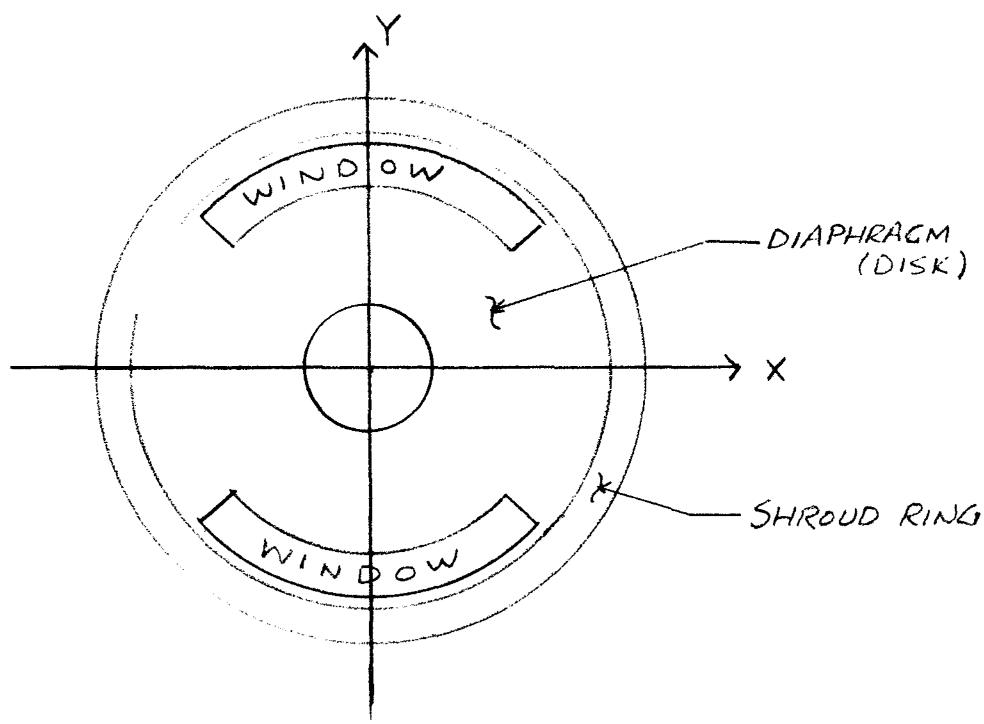

2. THICKNESS VARIATIONS THROUGH THE DISK CAN BE TREATED WITH AN EFFECTIVE MODULUS, I.E., MODULUS × THICKNESS, FOR AN IN-PLANE ANALYSIS

3. THE SHROUD CAN BE REPRESENTED BY AN EQUIVALENT RING BASED ON THERMAL EXPANSION AND STIFFNESS CHARACTERISTICS OF THE ACTUAL SHROUD RING.

01-071-002

QUADRILLE WORK SHEET

AEROJET-GENERAL CORPORATION
AZUSA, CALIFORNIA

DATE 12-1-66

SUBJECT 2ND STAGE NOZZLE DIAPHRAGM BY FPB WORK ORDER 7310-23-100 SNAP-8

BOUNDARY CONDITIONS

PLANE STRESS

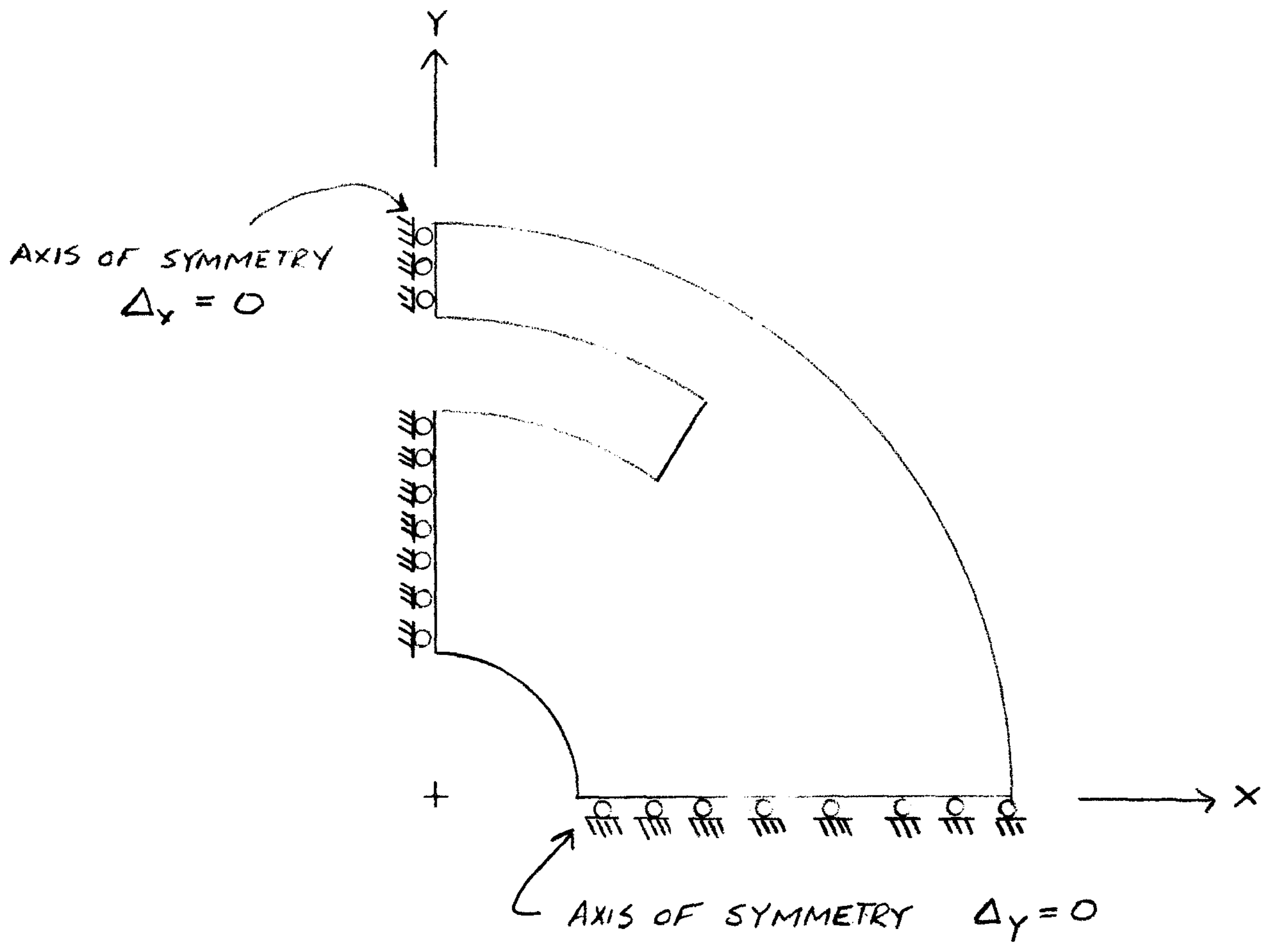

B.C.'S INPUT AT EACH NODAL POINT
ON AXES OF SYMMETRY

ALL OTHER BOUNDARY POINTS : FORCES = 0

FIGURE 12 - PLANE STRESS BOUNDARY CONDITIONS

01-071-002

AEROJET GENERAL TIRE GENERAL

AEROJET-GENERAL CORPORATION
AZUSA, CALIFORNIA

QUADRILLE WORK SHEET

PAGE 23 OF ____ PAGES
DATE 6 MAR 1967
SUBJECT 2ND STAGE NOZZLE DIAPHRAGM BY FPB WORK ORDER 7310·23·100
SNAP-8

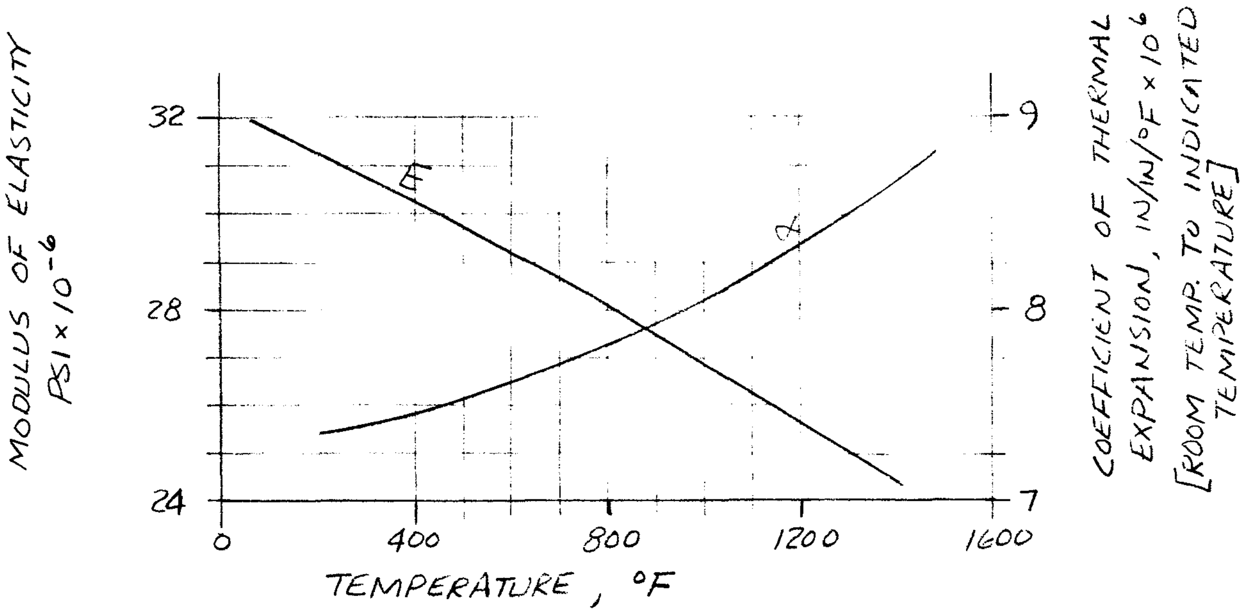

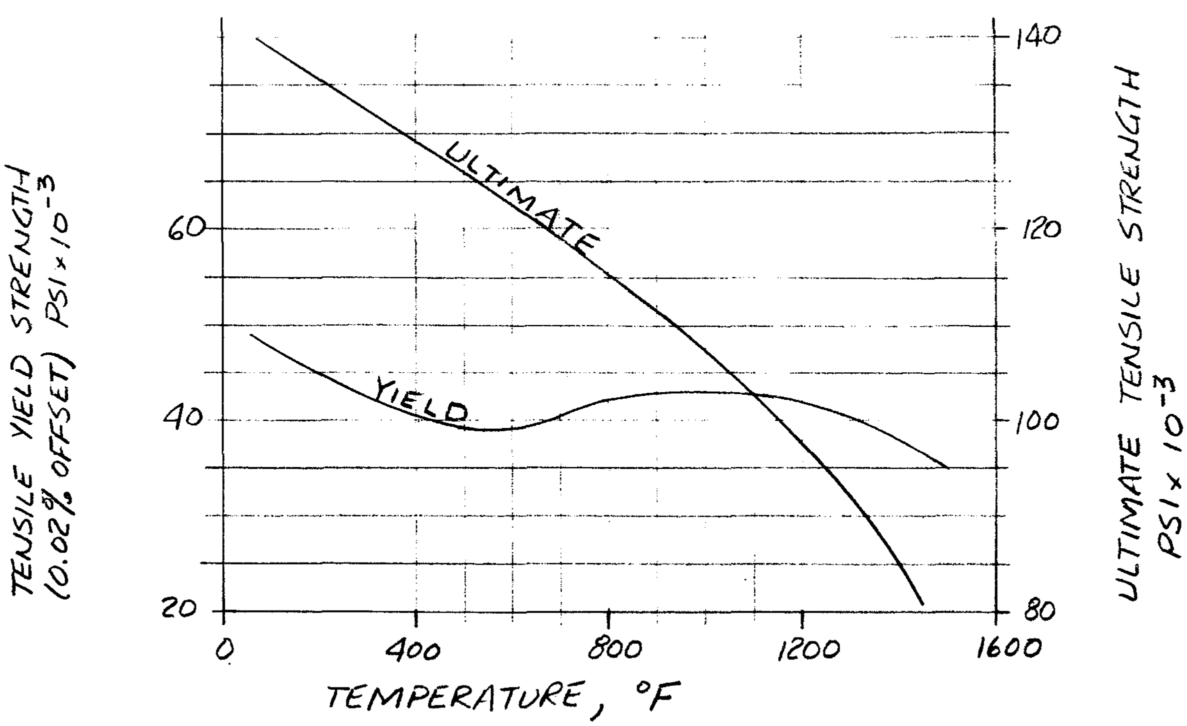

FIGURE 13 - MATERIAL PROPERTIES FOR S-816

SUBJECT 2ND STAGE NOZZLE DIAPHRAGM BY FPB
WORK ORDER 7310·23-100
SNAP-8

TABLE I ACTUAL AND EQUIVALENT MATERIAL PROPERTIES FOR ELEMENT THICKNESSES BASED ON S-816

EQUIVALENT VALUE = ACTUAL VALUE × THICKNESS

MATERIAL NUMBER †	ACTUAL				EQUIVALENT	
	TEMP °F	THICKNESS INCHES	E $PSI \times 10^{-6}$	F_{ty} $PSI \times 10^{-3}$	$\bar{E}$ $PSI \times 10^{-6}$	$\bar{F}_{ty}$ $PSI \times 10^{-3}$
1	400	0.30	30.5		9.15	
	800		28.0		8.40	
2	400	0.120	30.5		3.66	
	800		28.0		3.36	
3	400	0.360	30.5		11.0	
	800		28.0		10.1	
6	400	0.500	30.5		15.2	
	800		28.0		14.0	
4*	560				$\bar{E} = 18.4 \times 10^{6}$ PSI $\bar{\alpha} = 7.72 \times 10^{-6}$ IN/IN/°F	

* EQUIVALENT SHROUD RING (SEE PAGE)

† SEE FIGURE 5 FOR LOCATION OF MATERIALS

EQUIVALENT SHROUD RING - IN-PLANE ANALYSIS

SINCE BENDING EFFECTS ARE NEGLECTED IN THE IN-PLANE (PLANE STRESS) ANALYSIS, AN EQUIVALENT SHROUD RING IS USED TO REPRESENT THE IN-PLANE STIFFNESS OF THE ACTUAL SHROUD. THE EQUIVALENCE IS BASED ON THE DEFLECTION CHARACTERISTICS OF THE ACTUAL SHROUD RING AT THE INTERFACE OF THE SHROUD AND DIAPHRAGM DUE TO INTERFACE PRESSURE AND THERMAL LOADS.

INTERFACE PRESSURE ON FREE-BODY SHROUD

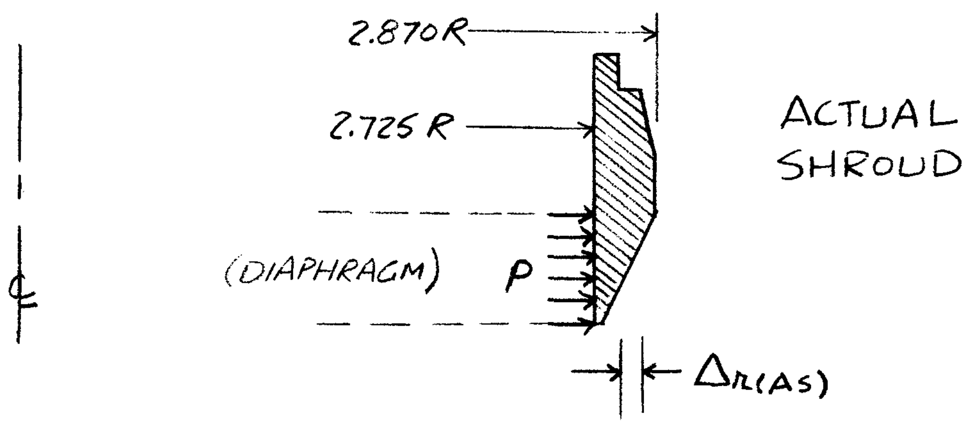

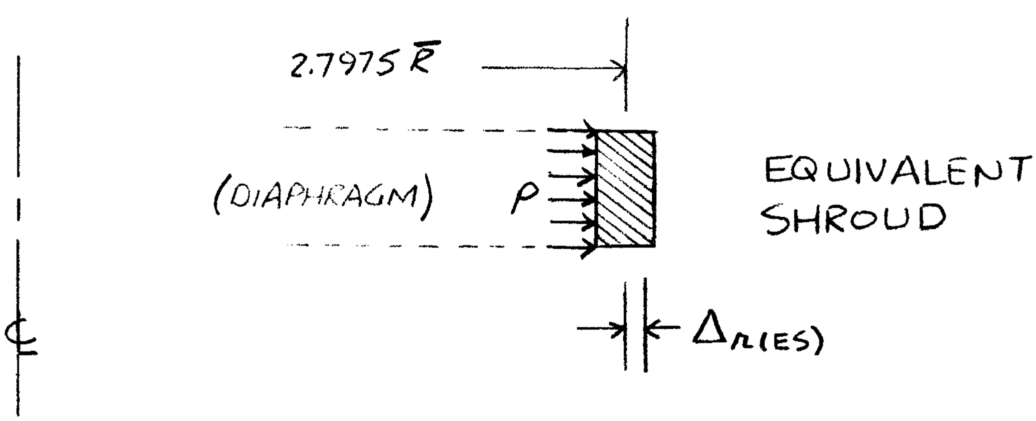

SUBJECT 2ND STAGE NOZZLE DIAPHRAGM BY FPB

WORK ORDER 7310·23·100
SNAP·8

RADIAL DISPLACEMENT OF EQUIVALENT SHROUD RING

$$\Delta_{r(ES)} = \frac{pR^2(1-\nu/2)}{E(R_2-R_1)}$$

$$= \frac{p(2.7975)^2(1-0.15)}{E(.145)}$$

$$= \frac{46.\,p}{E}$$

MAINTAINING THE RADIAL DISPLACEMENTS AND PRESSURES OF THE ACTUAL AND EQUIVALENT SHROUDS

$$P_{(AS)} = P_{(ES)} = 1000 \text{ psi}$$

$$\Delta_{r(AS)} = \Delta_{r(ES)} = 0.0025 \text{ IN.}$$

$$2.5\times10^{-3} = 46\times10^{3}/E$$

$$E = \frac{46\times10^{3}}{2.5\times10^{-3}} = \underline{18.4\times10^{6} \text{ PSI} \quad \text{EQUIVALENT } E}$$

THERMAL DISPLACEMENT OF FREE-BODY SHROUD

FOR AN EQUIVALENT SHROUD (DISK) OF CONSTANT TEMPERATURE

$$u_{r(ES)} \text{ [@ INNER RADIUS]} = 2.725\,\alpha\,T_c$$

FOR $T_c = 560-80 = 480°F$

AND $u_{r(AS)} = 0.0102$ IN

$$\alpha = \frac{10.2\times10^{-3}}{2.725(480)} = \underline{7.72\times10^{-6} \text{ IN/IN/°F} \quad \text{EQUIVALENT } \alpha}$$

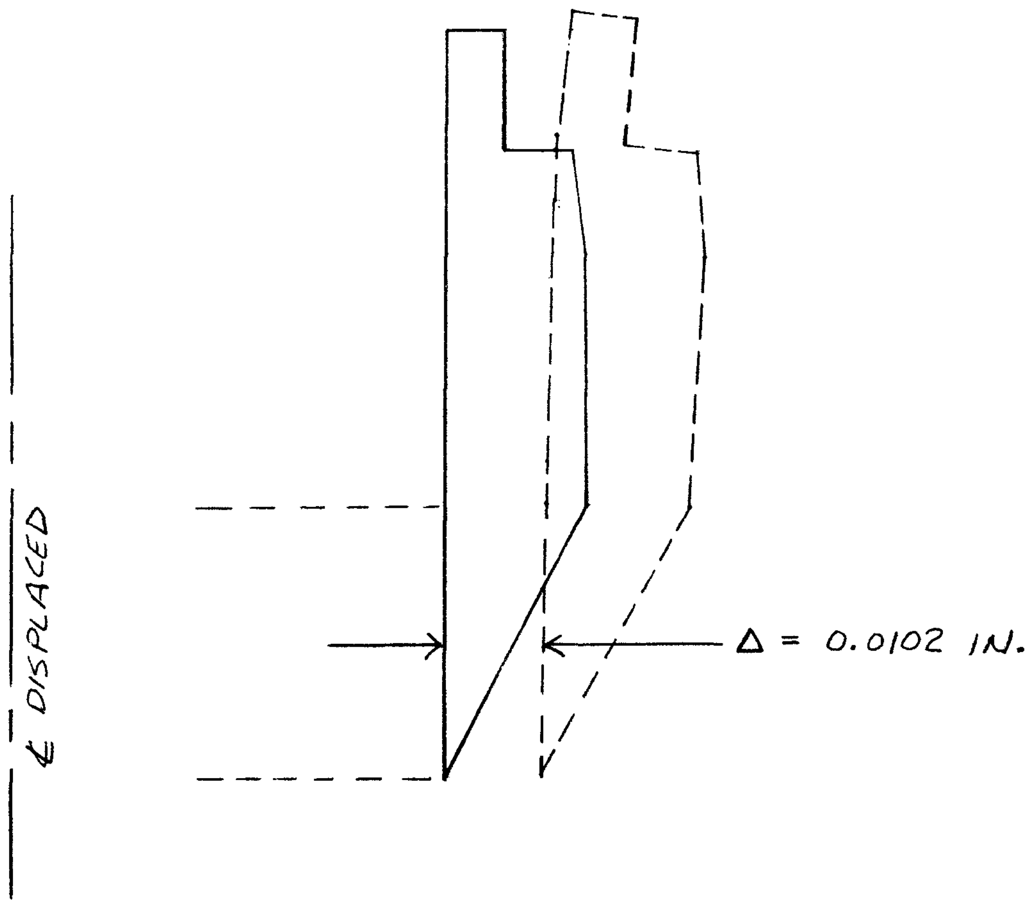

FIGURE 14 - DISPLACEMENT OF FREE-BODY SHROUD (AXISYMMETRIC) FOR THERMAL CONDITION

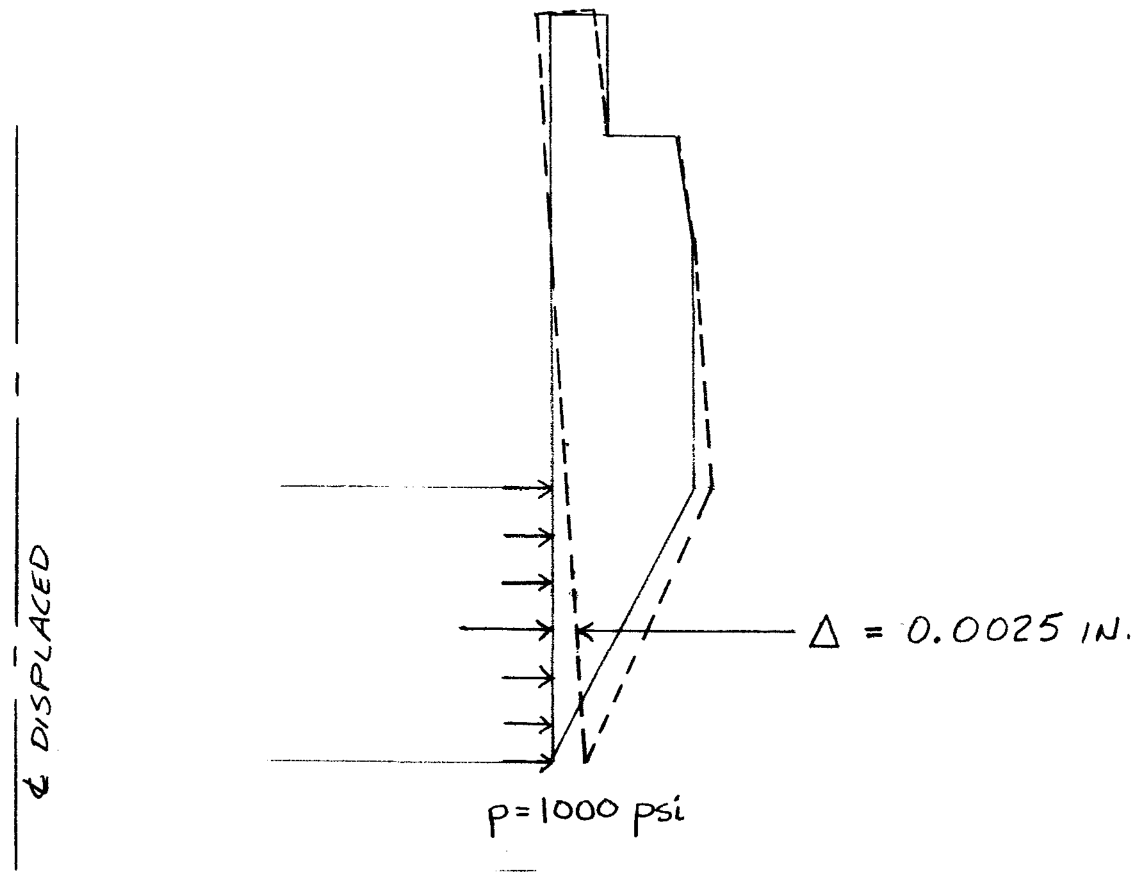

FIGURE 15 - DISPLACEMENT OF FREE-BODY SHROUD (AXISYMMETRIC) FOR INTERFACE PRESSURE CONDITION

FIGURE 16 - BENDING - BOUNDARY CONDITIONS

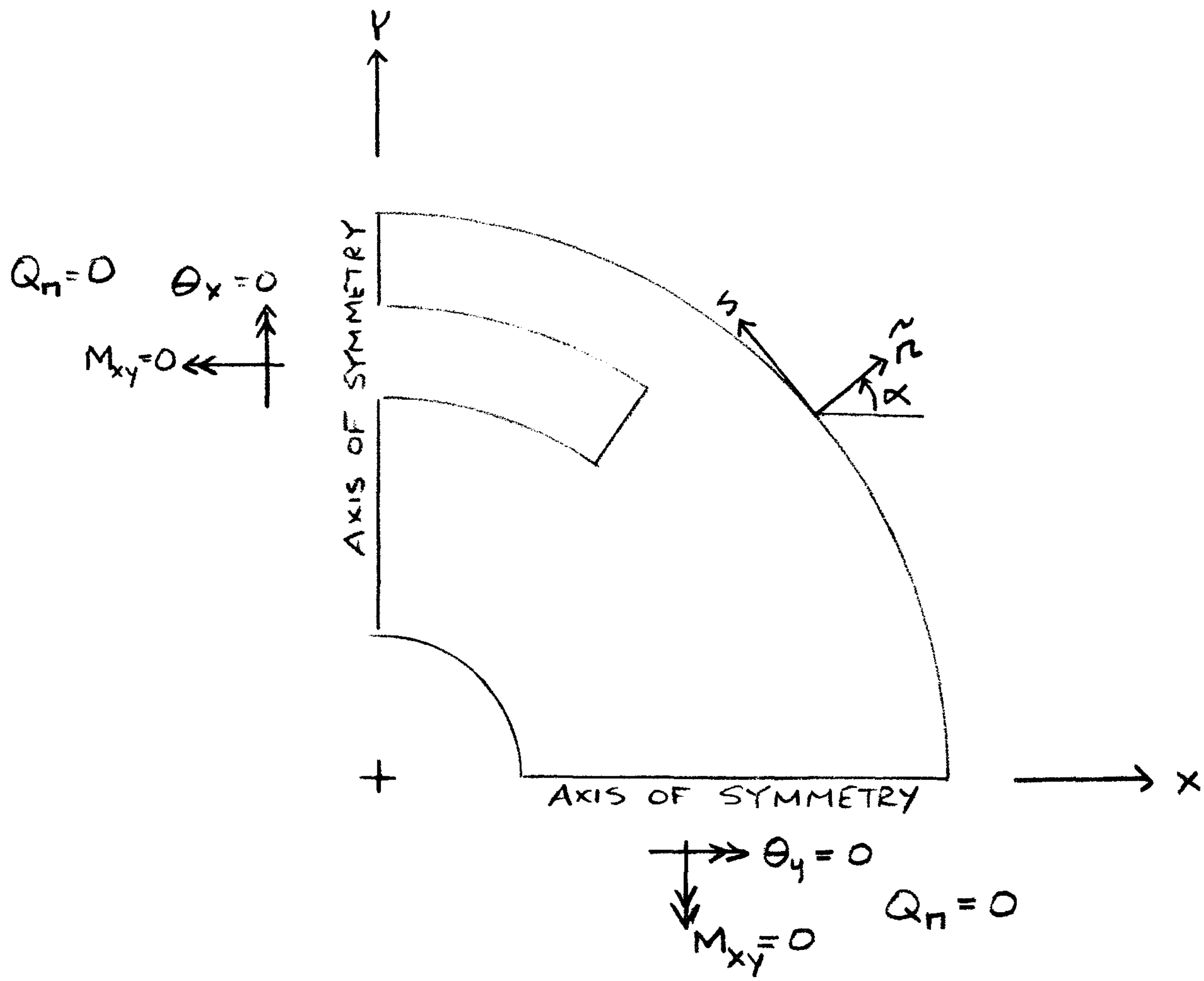

B.C.'S INPUT AT EACH NODAL ON BOUNDARIES.
B.C.'S IN TERMS OF A REFERENCE $\tilde{n}$, s AXES

FOR FREE EDGE ; $M_{\tilde{n}} = 0$, $M_{\tilde{n}s} = 0$, $Q_n = 0$

FOR SIMPLY SUPPORTED ; $M_{\tilde{n}} = 0$, $M_{\tilde{n}s} = 0$, $w_n = 0$

SUBJECT 2ND STAGE NOZZLE DIAPHRAGM BY FPB WORK ORDER 7310·23·100
SNAP·8

THERMAL BENDING

DUE TO TEMP. GRADIENT ACROSS THICKNESS OF DISK

SINCE THE THERMAL DEFLECTION PATTERN OF THE SHROUD (TEMP. CONDITION REMOTE FROM THE WINDOW AREA) SHOWS ESSENTIALLY A ZERO SLOPE ALONG THE INNER RADIUS OF THE SHROUD RING (WHERE THE DISK IS AN INTEGRAL PART OF THE STRUCTURE) THE THERMAL BENDING CASE IS RUN FOR NO THERMAL BENDING MOMENT ON THE SHROUD.

THERMAL MOMENTS ARE INPUT ON EACH ELEMENT DETERMINED FROM THE FOLLOWING

$$m_T = \int_{-h/2}^{h/2} E\alpha T z \, dz$$

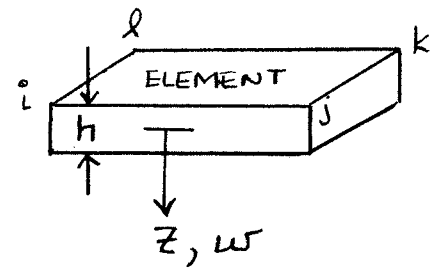

i, j, k, l NODAL POINTS

FOR A LINEAR GRADIENT

$$m_T = -E\alpha\left[\frac{h^2}{12}(\Delta T)\right]$$

WHERE ΔT = (UPSTREAM TEMP − DOWNSTREAM TEMP), °F.

QUADRILLE WORK SHEET

AEROJET GENERAL TIRE GENERAL

AEROJET-GENERAL CORPORATION
AZUSA, CALIFORNIA

DATE 17 MAR 1967

SUBJECT 2ND STAGE NOZZLE DIAPHRAGM BY FPB WORK ORDER 7310·23·100
SNAP·8

FOR T_{AVG} (THROUGH THE THICKNESS) = 600°F

$$E = 29 \times 10^6 \text{ PSI}$$
$$\alpha = 7.7 \times 10^{-6} \text{ IN/IN/°F}$$

$$m_T = -\frac{29(7.7)}{12}\Delta T = -18.6\,\Delta T$$

THE FOLLOWING TABLE IS CONSTRUCTED TO CONVERT THE ΔT'S FROM THE CONTOUR PLOT IN FIGURE 9 TO m_T (THERMAL MOMENT)

ΔT	m_T	
	$h = 0.30$	$h = 0.36$
130	-217	
160	-267	
200	-334	
225	-380	
250	-427	
300	-500	-720

01-071-002

AEROJET-GENERAL CORPORATION
AZUSA, CALIFORNIA

QUADRILLE WORK SHEET

PAGE 32 OF ____ PAGES
DATE 14 MAR 1967
WORK ORDER 7310.23.100
SNAP-8

SUBJECT 2ND STAGE NOZZLE DIAPHRAGM BY FPB

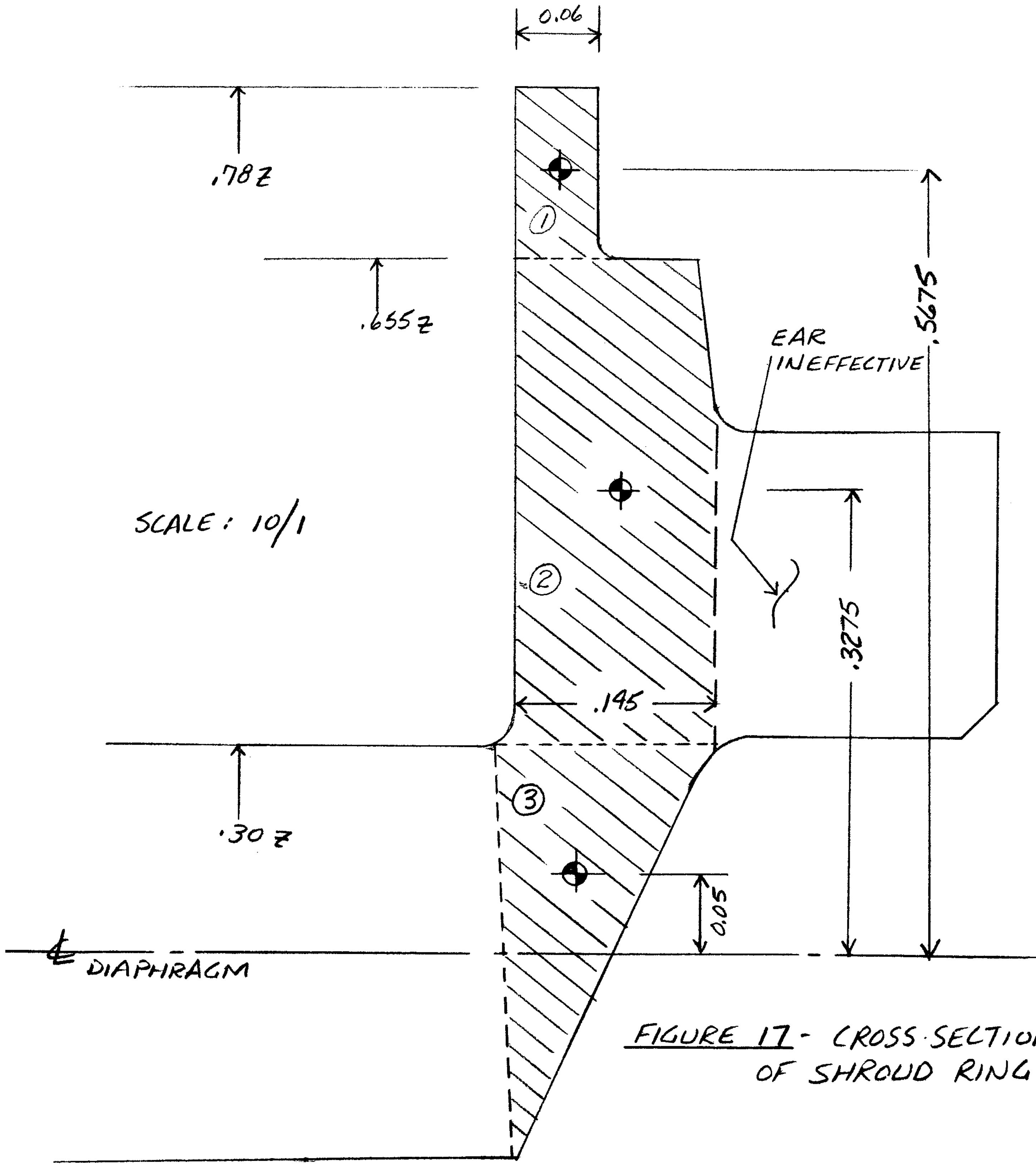

FIGURE 17 - CROSS SECTION OF SHROUD RING

MOMENT OF INERTIA
AND EQUIVALENT THICKNESS OF THE SHROUD

SEE FIGURE

① $I_1 = \frac{bh^3}{12} + Ad^2$

$= \frac{.06(.125)^3}{12} + (.06)(.125)(.5675)^2$

$= .00000977 + .00241 = \underline{0.0024198 \text{ IN}^4}$

② $I_2 = \frac{.145(.355)^3}{12} + (.145)(.355)(.3275)^2$

$= .000541 + .00552 = \underline{0.00606 \text{ IN}^4}$

③ $I_3 = \frac{bh^3}{36} + Ad^2$

$= \frac{.145(.30)^3}{36} + (.145)(.15)(.05)^2$

$= .0001085 + .0000545 = \underline{0.0001630 \text{ IN}^4}$

MOMENT OF INERTIA WITHOUT CUTS FOR VANES, I_A

$I_A = I_1 + I_2 + I_3 = 0.008643$

h_A (HEIGHT OF EQUIVALENT RECTANGLE @ ℄) $= \sqrt[3]{12\frac{I}{b}}$

$h_A = \sqrt[3]{\frac{12(.008643)}{.145}} = \sqrt[3]{.715} = .894 \text{ IN} \leftarrow$

MOMENT OF INERTIA WITH CUTS FOR VANES, I_B

$I_B = I_1 + I_2 = 0.00848$

$h_B = \sqrt[3]{\frac{12(.00848)}{.145}} = \sqrt[3]{.702} = .889 \text{ IN.} \leftarrow$

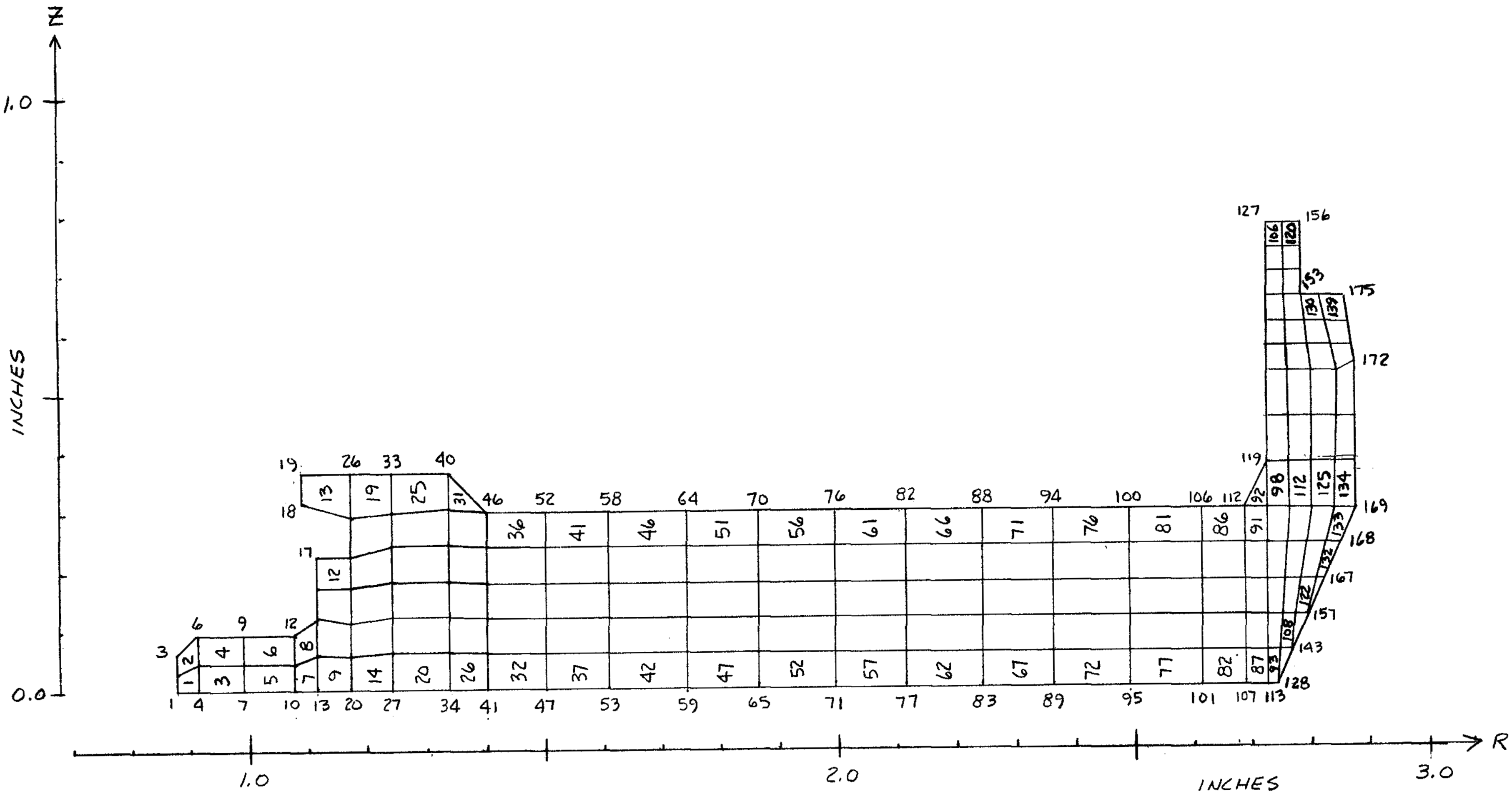

FIGURE 18
FINITE ELEMENT GRID
FOR AXISYMMETRIC CASE

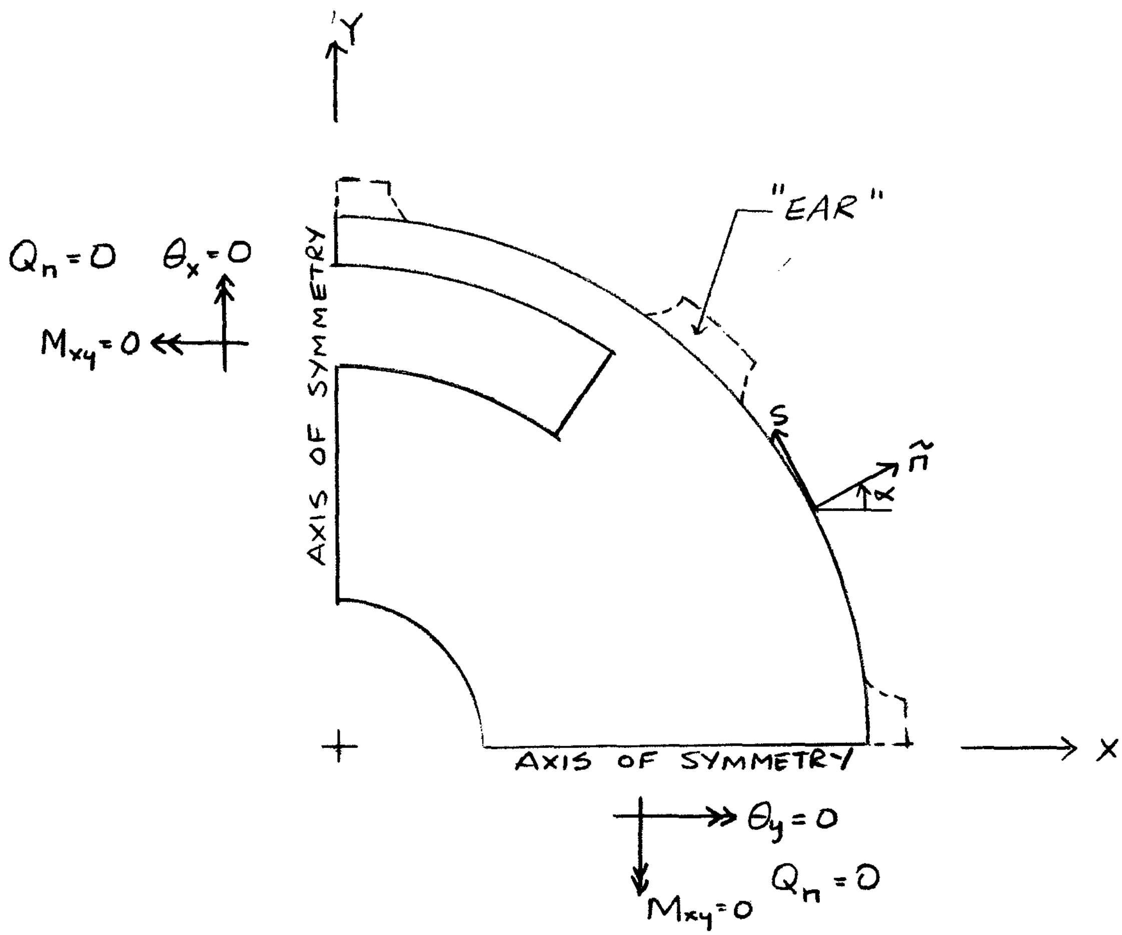

BOUNDARY CONDITIONS

a) INPUT AT EACH NODAL POINT ON BOUNDARIES

b) IN TERMS OF A REFERENCE $\tilde{n}$, S AXIS

c) FOR FREE EDGE, $M_{\tilde{n}} = 0$, $M_{\tilde{n}s} = 0$, $Q_n = 0$

d) FOR NODAL POINTS LOCATED AT "EARS"
$M_{\tilde{n}} = 0$, $M_{\tilde{n}s} = 0$, $\omega_n = 0$

FIGURE 19 - BOUNDARY CONDITIONS FOR BENDING SOLUTION WITH NORMAL PRESSURE

PRESSURE AREA = .483 SQ.IN.
PRESSURE = 75 PSI
TOTAL LOAD TRANSFERRED TO WINDOW EDGES BY VANES = 36.2 LBS

ASSUME HALF OF LOAD TO EACH EDGE

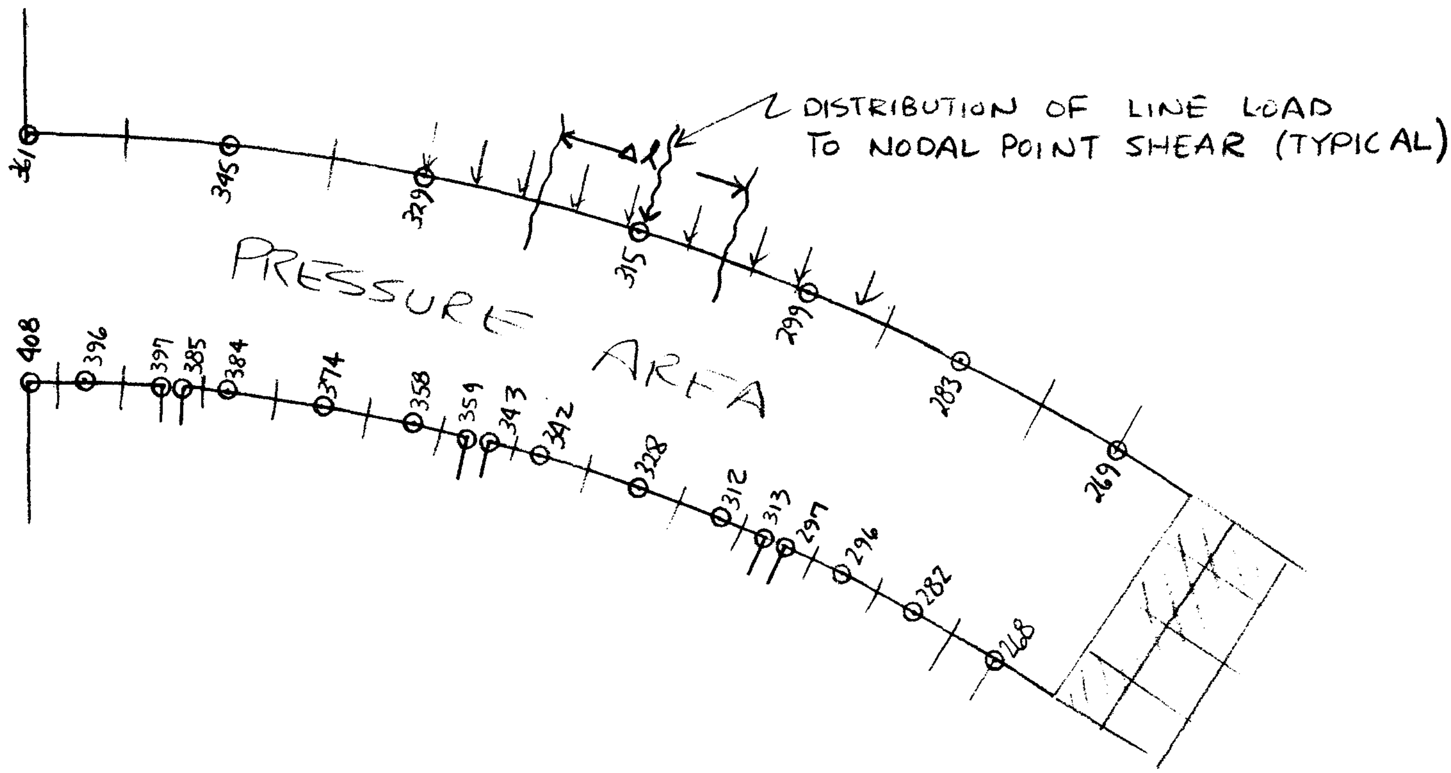

SCALE – 4:1

FIGURE 20 – SHEAR LOADS ON WINDOW NODAL POINTS

QUADRILLE WORK SHEET

AEROJET GENERAL

AEROJET-GENERAL CORPORATION
AZUSA, CALIFORNIA

DATE 11-29-66

SUBJECT 2ND STAGE NOZZLE DIAPHRAGM BY FPB WORK ORDER 7310-23-100
SNAP-8

CALCULATION OF SHEAR LOADS ON WINDOW POINTS

NODAL POINT	$\Delta \ell$ (MEASURED)	$\Delta\ell/\ell$ × 18.1 LBS
268	.25	.9125
282	.45	1.6425
296	.38	1.387
297	.17	.6205
313	.13	.4745
312	.35	1.2775
328	.50	1.825
342	.39	1.4235
343	.13	.4745
359	.13	.4745
358	.39	1.4235
374	.49	1.7885
384	.39	1.4235
385	.10	.365
397	.21	.7665
396	.34	1.241
CORNER 408	.16	.584
	$4.96 = \ell$	18.106

$\frac{18.1}{4.96} = 3.65$ #/in

269	.45	1.37
283	.90	2.74
299	.90	2.74
315	1.00	3.05
329	1.09	3.32
345	1.09	3.32
CORNER 361	.51	1.55
	5.94	18.09

$\frac{18.1}{5.94} = 3.05$

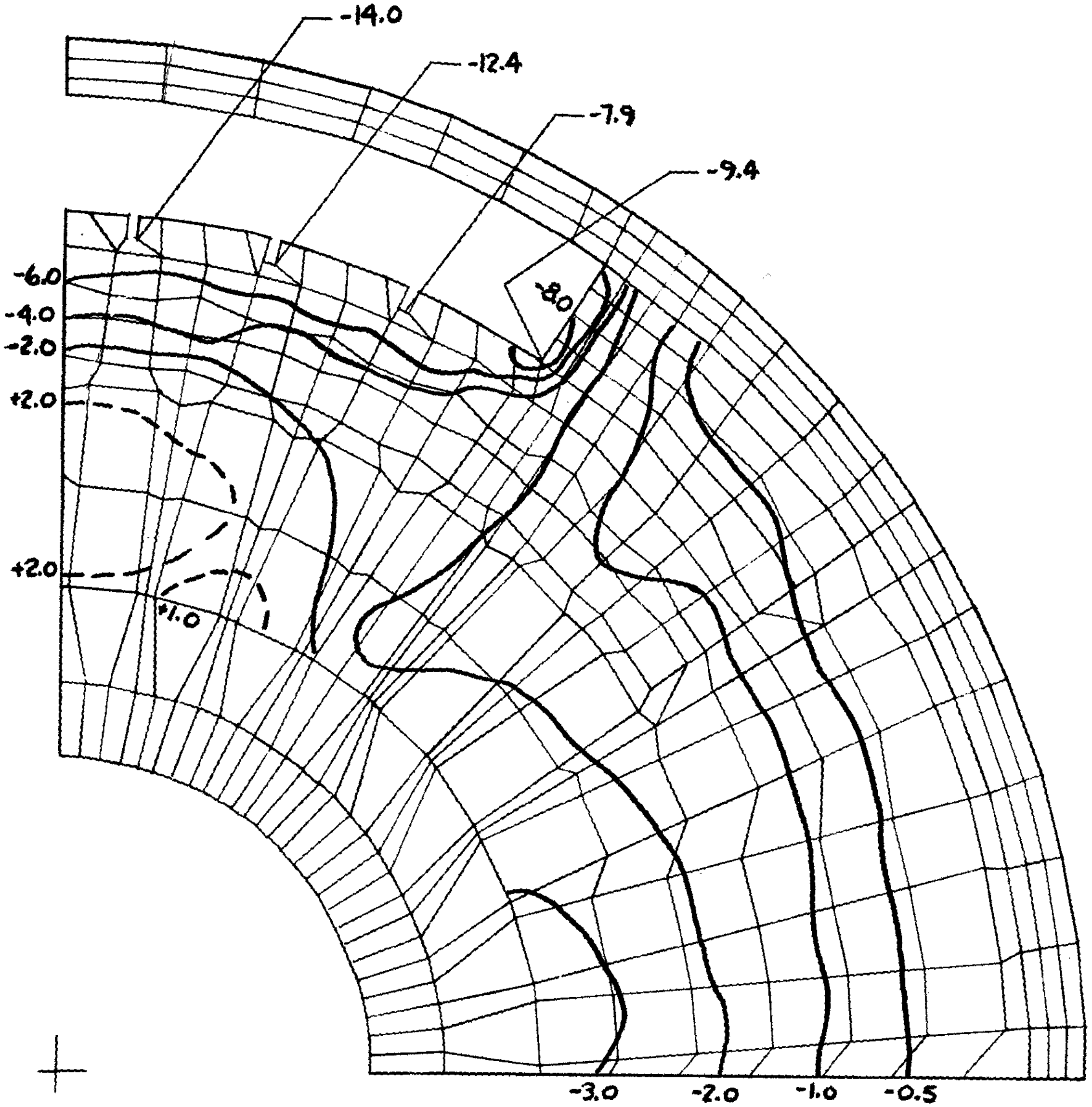

STRESS CONTOURS IN KSI
− = COMPRESSION
+ = TENSION

FIGURE 21
MAXIMUM PRINCIPAL STRESSES DUE TO IN-PLANE, THERMAL GRADIENTS

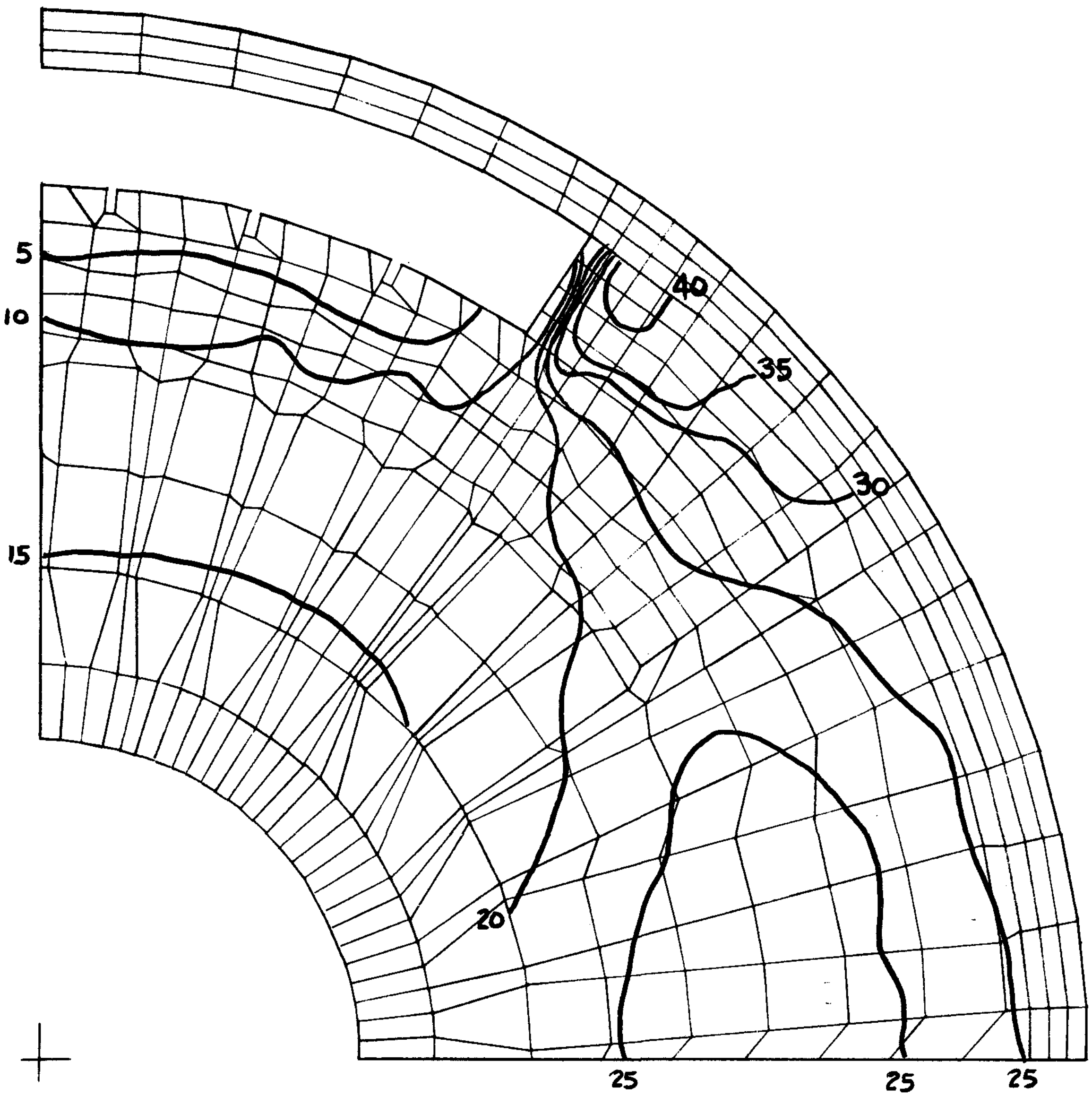

FIGURE 22

MAXIMUM PRINCIPAL STRESSES DUE TO THERMAL BENDING

STRESS CONTOURS IN KSI

SIGN OF STRESS IS

(−) COMPRESSION ON UPSTREAM FACE

(+) TENSION ON DOWNSTREAM FACE

SUBJECT 2ND STAGE NOZZLE DIAPHRAGM BY FPB

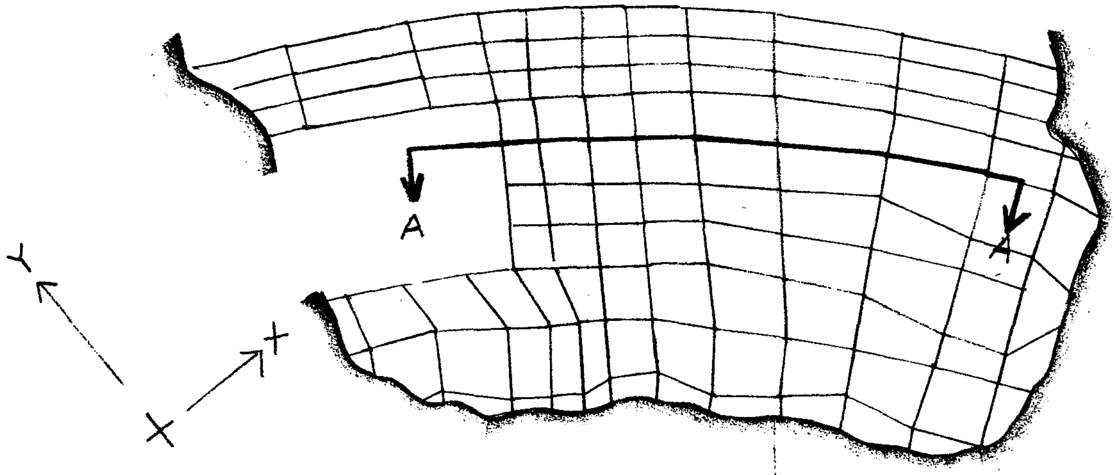

a) REGION OF MAXIMUM STRESS [FROM FIGURES 21 AND 22)

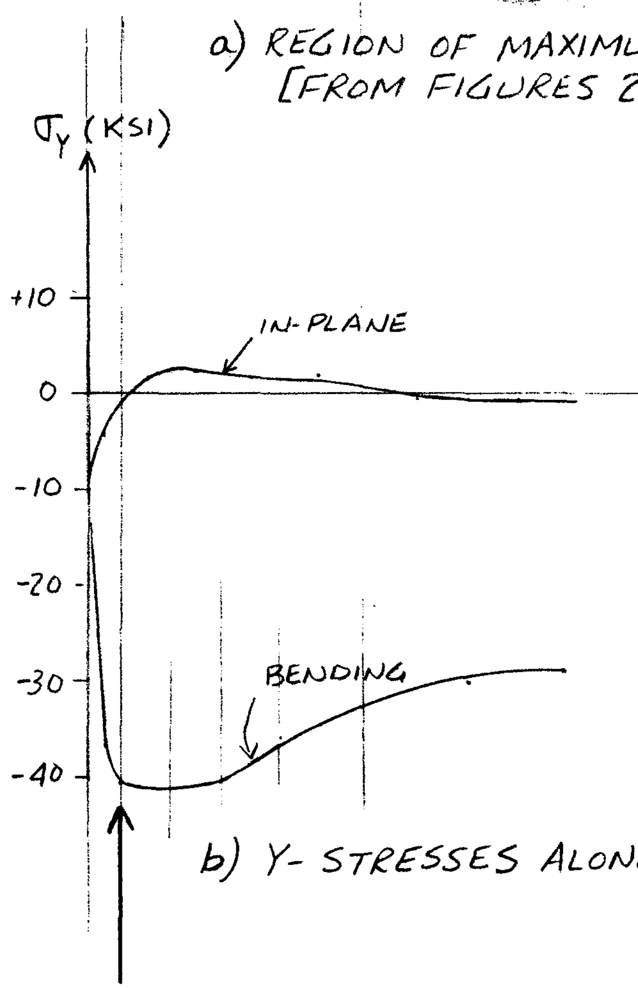

b) Y- STRESSES ALONG SECTION A-A

FIGURE 23 - STRESS COMPONENTS AT CRITICAL SECTION A-A

AEROJET GENERAL TIRE GENERAL
AEROJET-GENERAL CORPORATION
AZUSA, CALIFORNIA

QUADRILLE WORK SHEET

PAGE 41 OF ___ PAGES
DATE 20 MAR 1967
SUBJECT 2ND STAGE NOZZLE DIAPHRAGM BY FPB
WORK ORDER 7310.23.100
SNAP-8

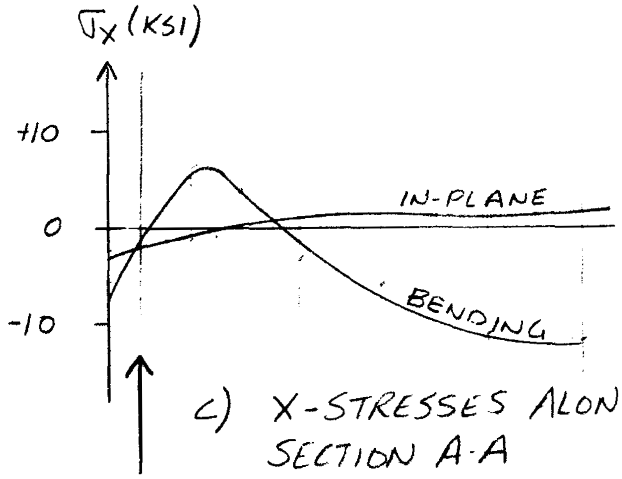

c) X-STRESSES ALONG SECTION A-A

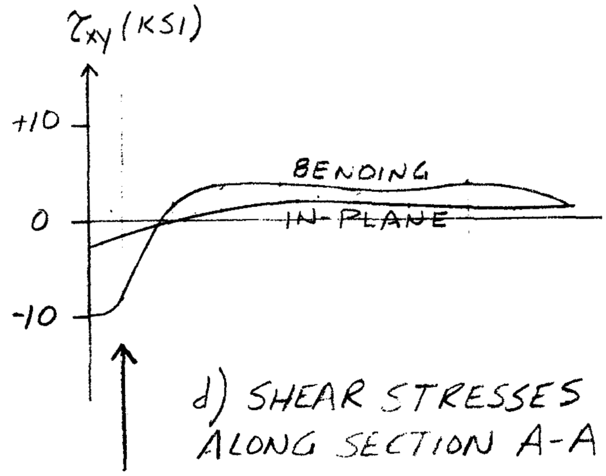

d) SHEAR STRESSES ALONG SECTION A-A

	σ_y	σ_x	τ_{xy}
IN-PLANE	- 1.5	-2.0	- 2.0
BENDING	-42.0	-8.0	-8.0
Σ	-43.5	-10.0	-10.0

MAXIMUM COMBINED PRINCIPAL STRESS (IN-PLANE + BENDING)

$$\sigma_{MAX} = \frac{\sigma_x + \sigma_y}{2} \pm \sqrt{\left(\frac{\sigma_x - \sigma_y}{2}\right)^2 + \tau_{xy}^2}$$

$$= -26.75 \pm \sqrt{380}$$

$$= -46.25 \text{ KSI}$$

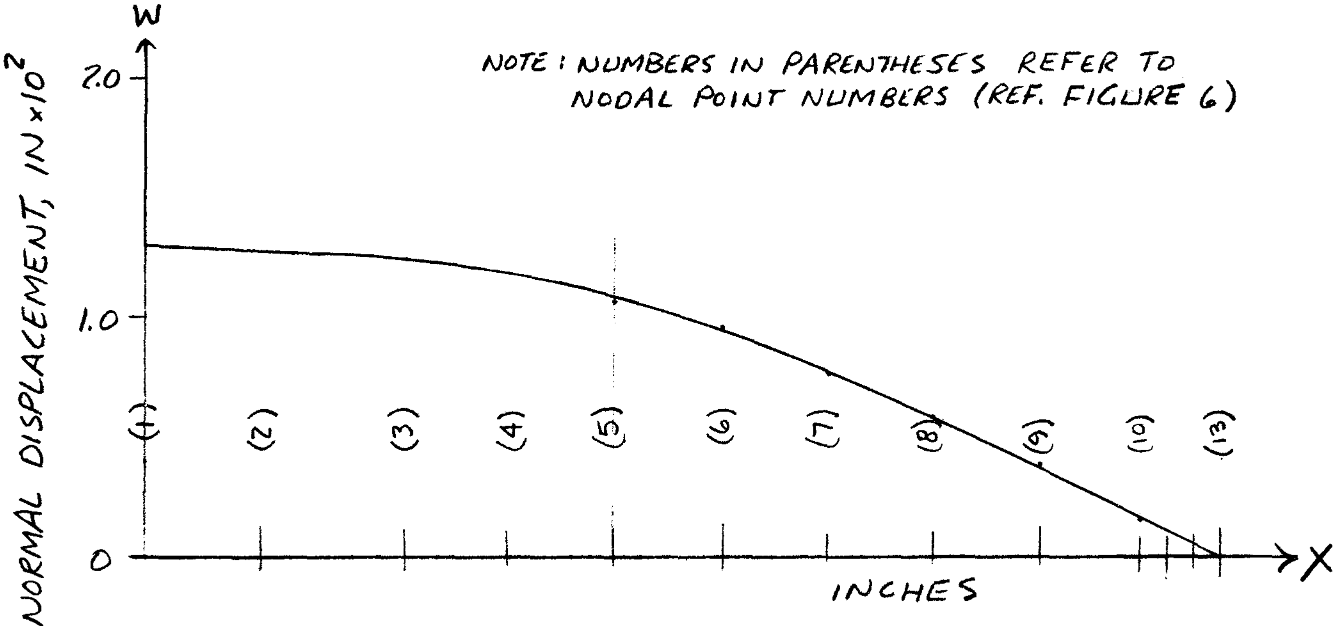

a) ALONG BOUNDARY Y = 0

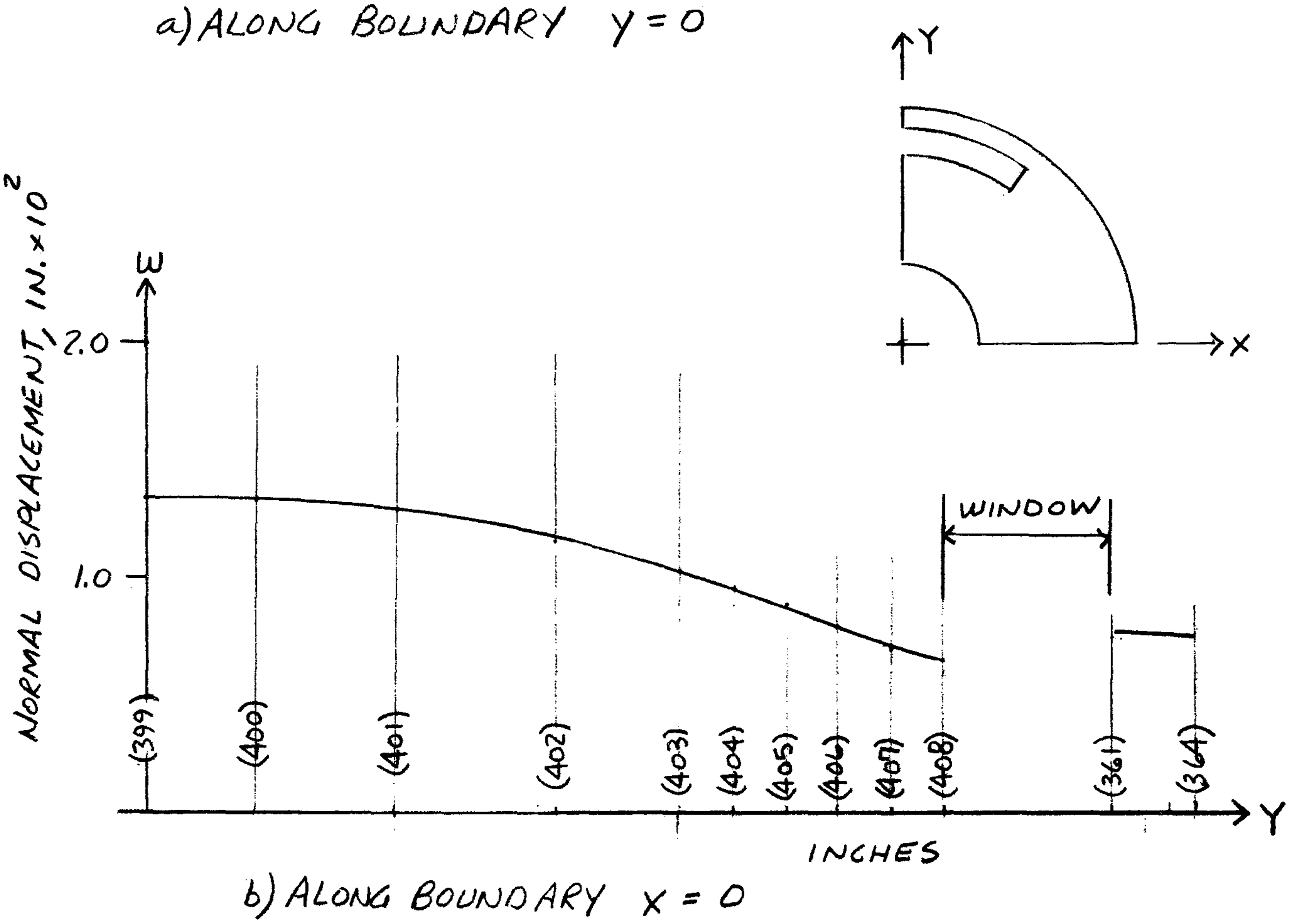

b) ALONG BOUNDARY X = 0

FIGURE 24 - NORMAL DISPLACEMENTS FOR THERMAL BENDING CASE

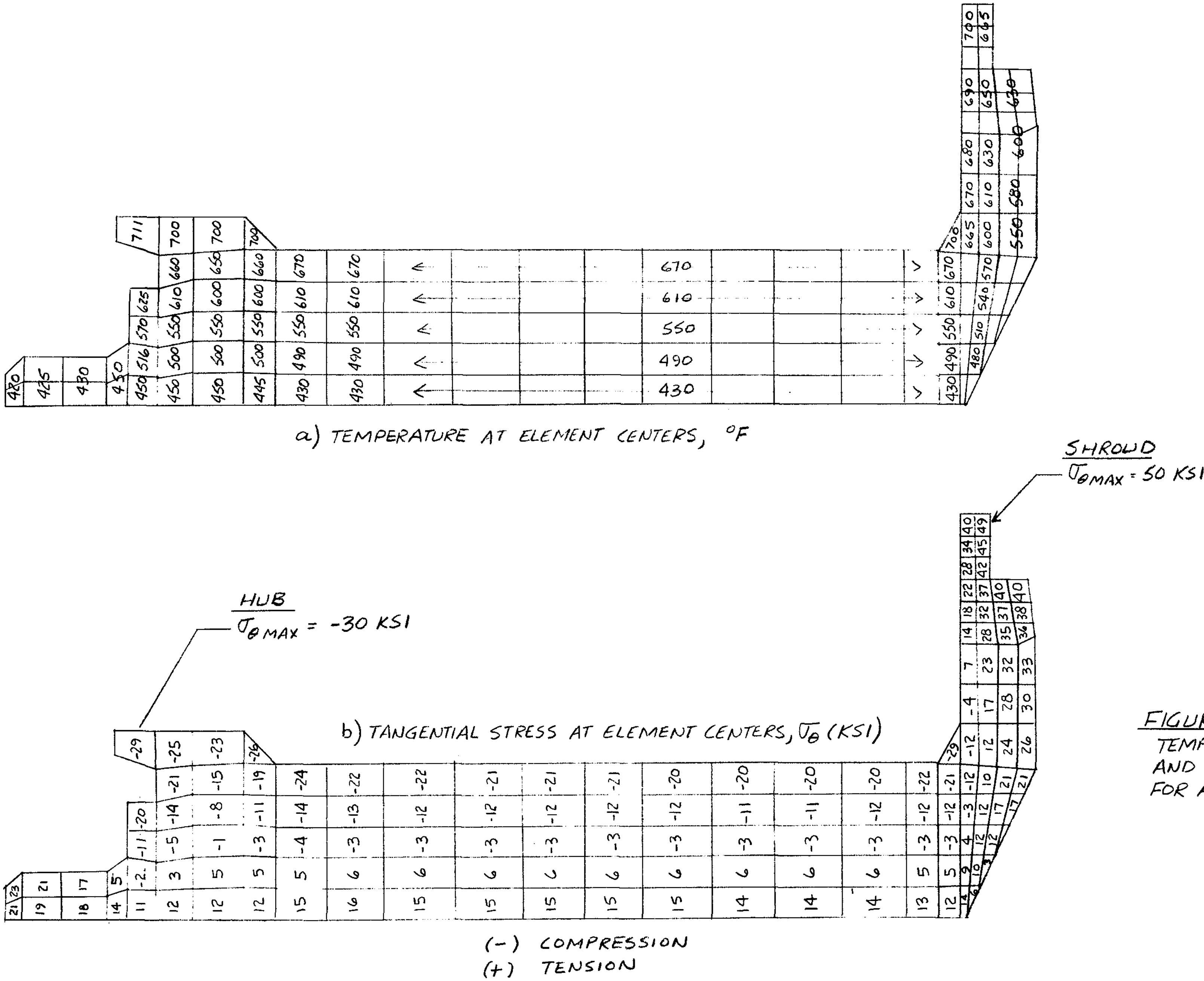

FIGURE 25
TEMPERATURE DISTRIBUTION AND TANGENTIAL STRESSES FOR AXISYMMETRIC CASE

01-071-002

QUADRILLE WORK SHEET

AEROJET-GENERAL CORPORATION
AZUSA, CALIFORNIA

DATE 20 MAR 1967

SUBJECT 2ND STAGE NOZZLE DIAPHRAGM BY FPB WORK ORDER 7310·23·100 SNAP-8

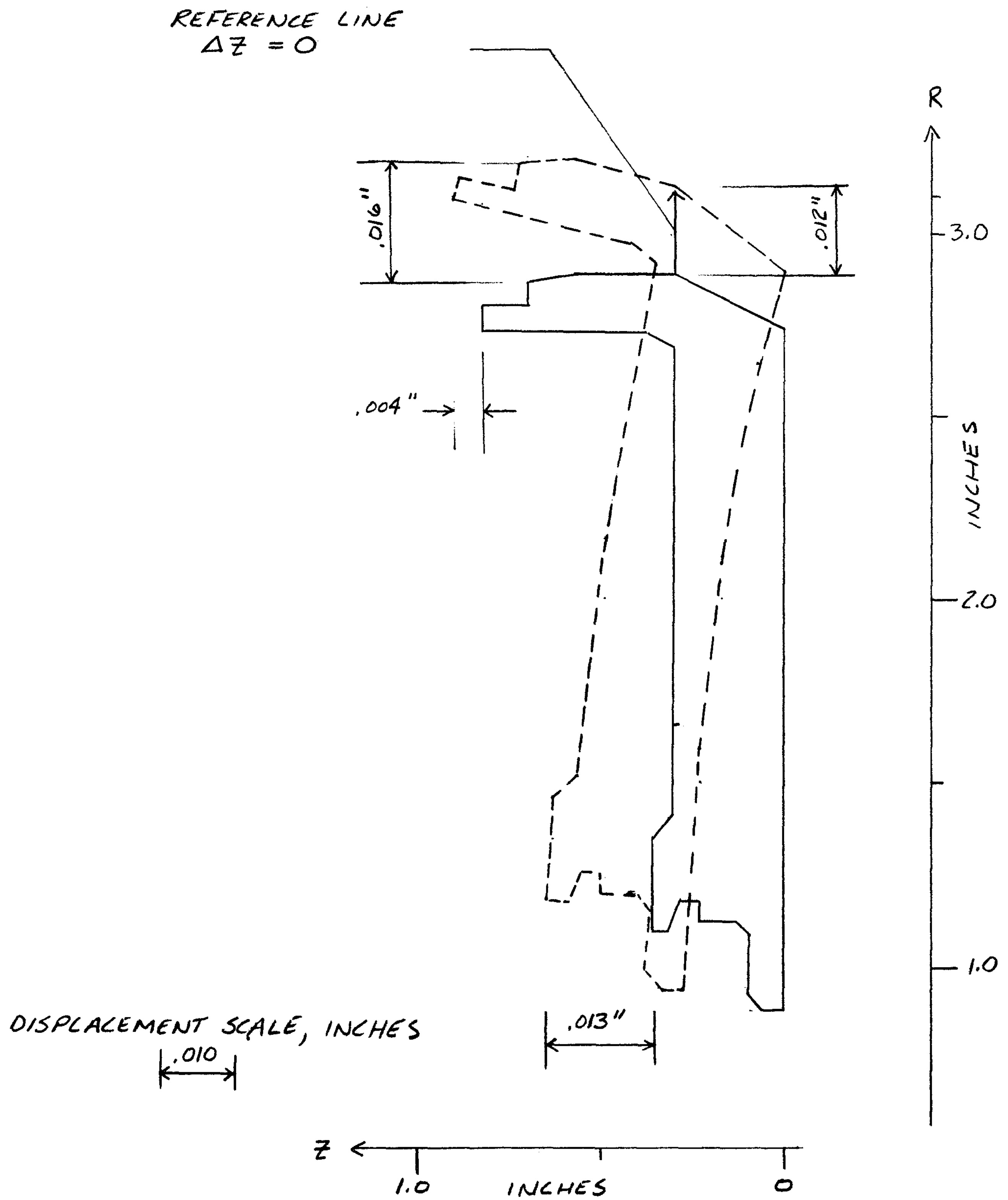

FIGURE 26 DISPLACEMENTS DUE TO AXISYMMETRIC THERMAL CASE

FIGURE 27
MAXIMUM PRINCIPAL STRESSES
DUE TO NORMAL PRESSURE
LOADING

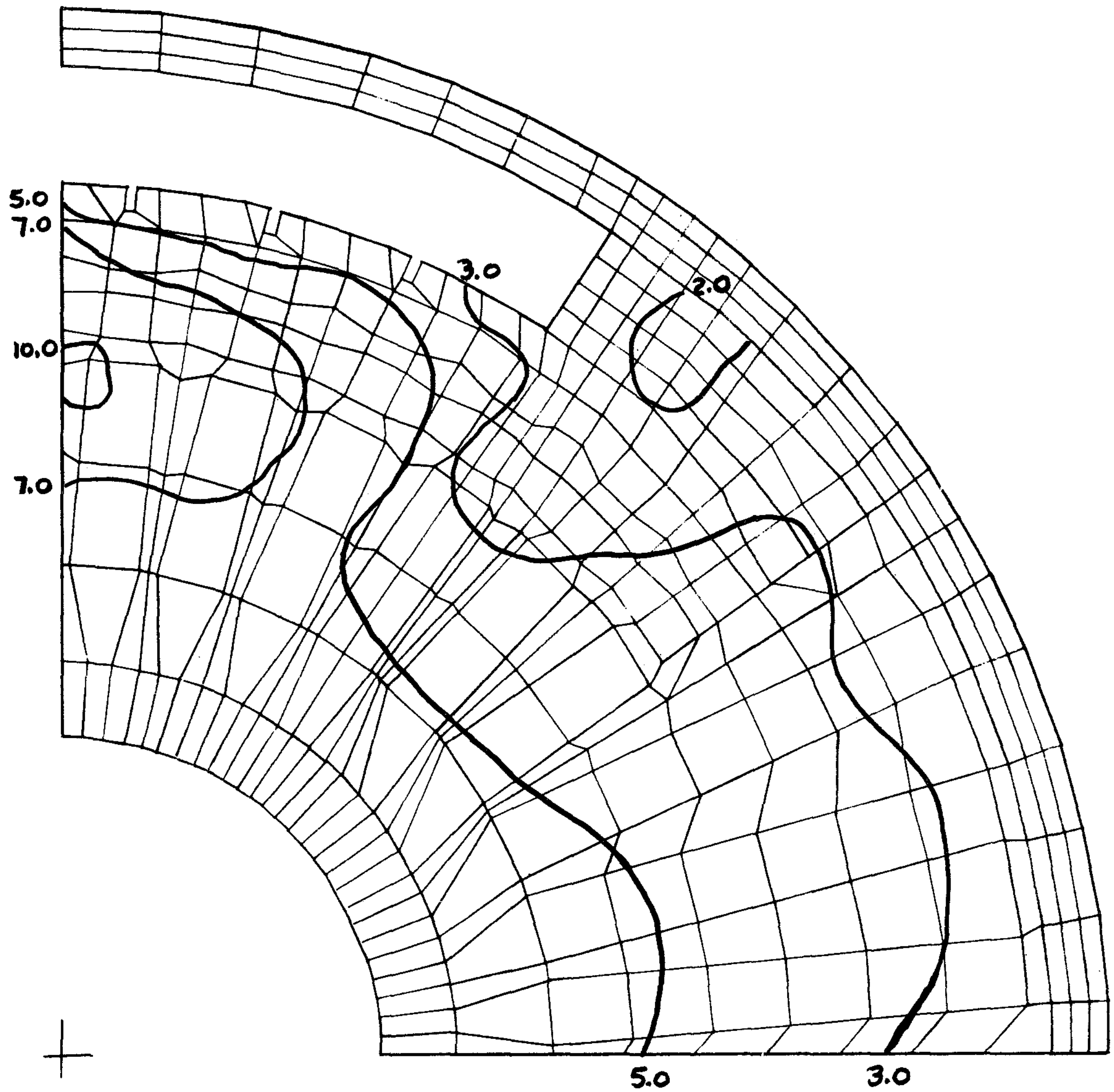

STRESS CONTOURS IN KSI
SIGN OF STRESS IS
(−) COMPRESSION ON UPSTREAM FACE
(+) TENSION ON DOWNSTREAM FACE

QUADRILLE WORK SHEET

AEROJET-GENERAL CORPORATION
AZUSA, CALIFORNIA

PAGE 46 OF ____ PAGES
DATE 20 MAR 1967
SUBJECT 2ND STAGE NOZZLE DIAPHRAGM BY FPB
WORK ORDER 7310.23.100
SNAP.8

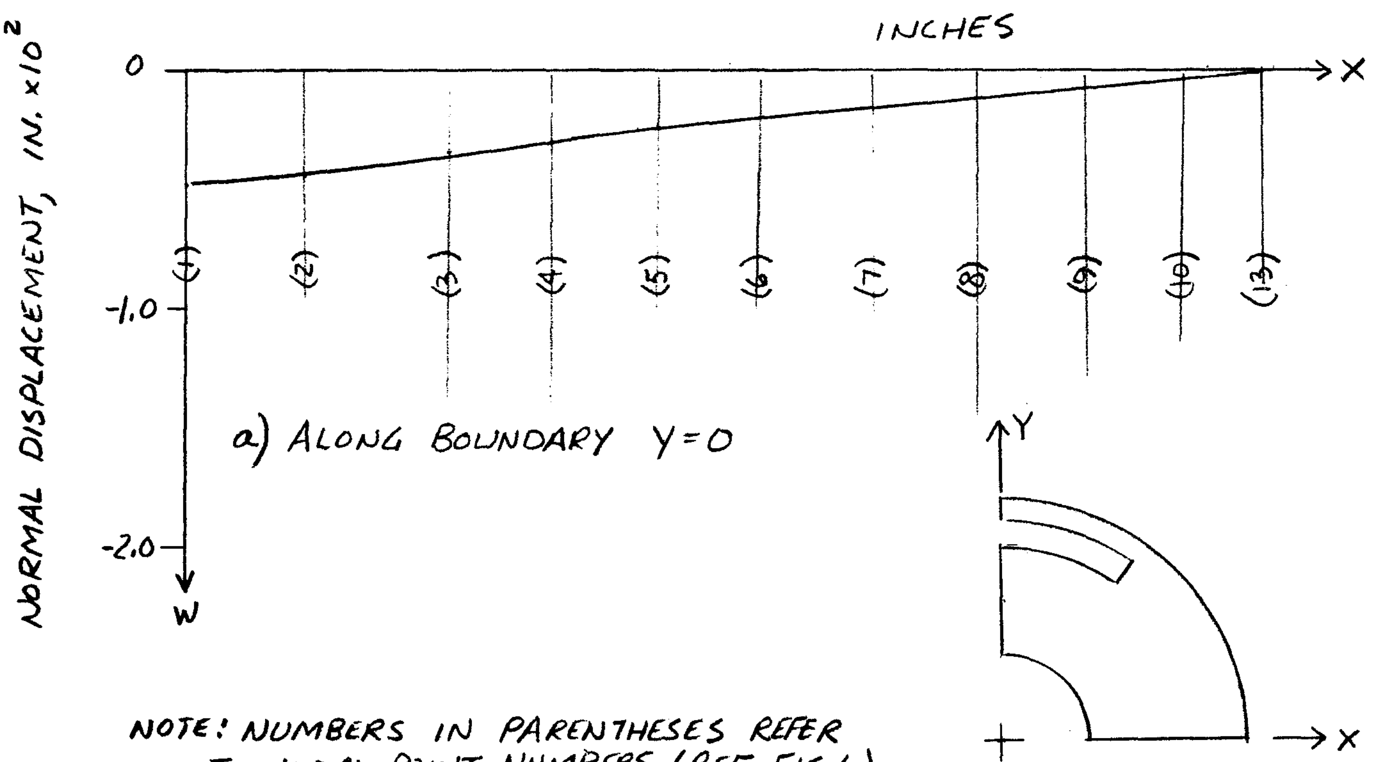

a) ALONG BOUNDARY Y=0

NOTE: NUMBERS IN PARENTHESES REFER TO NODAL POINT NUMBERS (REF. FIG.6)

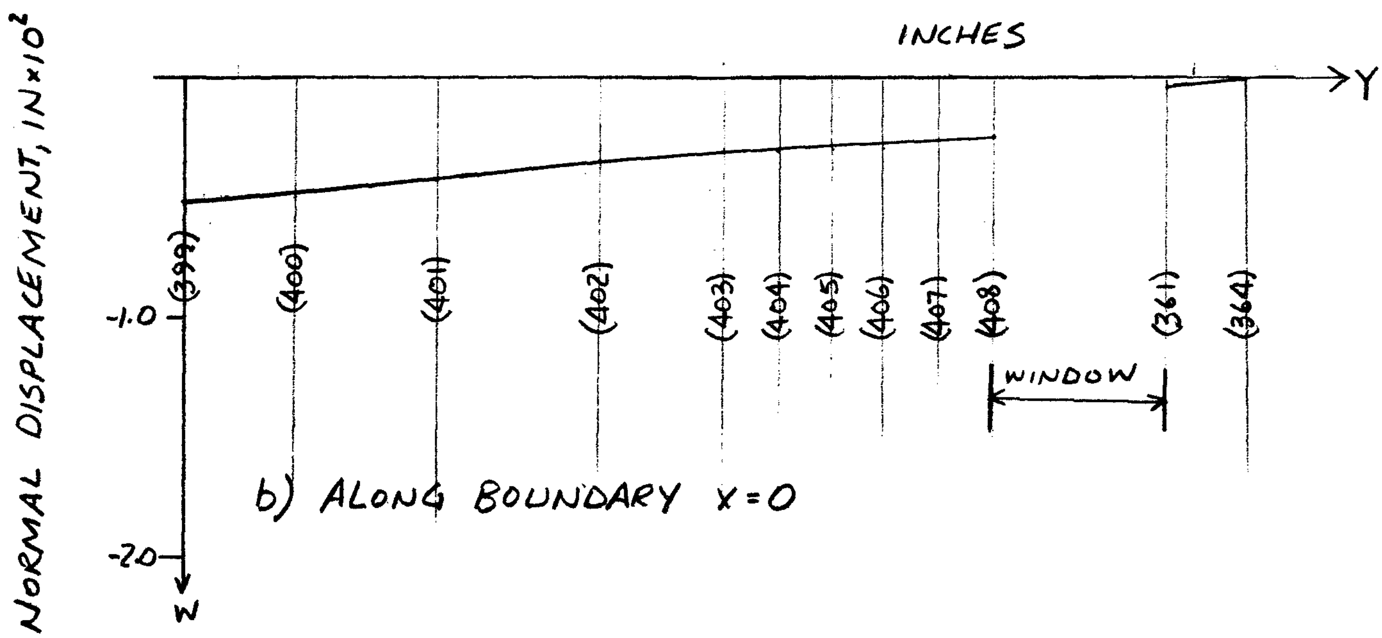

b) ALONG BOUNDARY X=0

FIGURE 28 – NORMAL DISPLACEMENTS FOR PRESSURE LOADING CASE

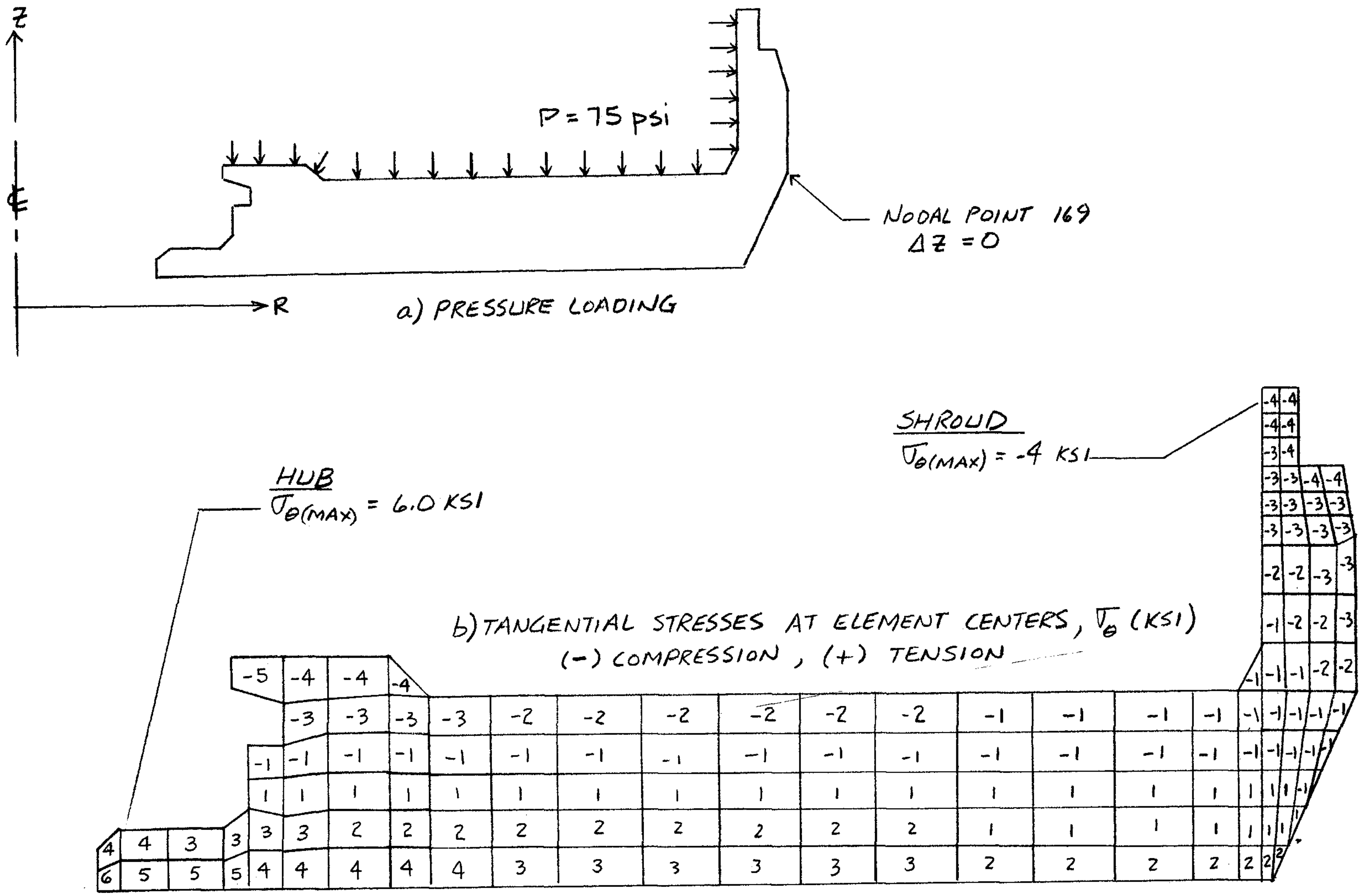

FIGURE 29
TANGENTIAL STRESSES DUE TO NORMAL PRESSURE LOADING FOR AXISYMMETRIC CASE

VI. REFERENCES

1. Zienkiewicz, O. C. and Holister, G. S., Stress Analysis, Chapters 7, 8 and 9, John Wiley and Sons Ltd., London, 1965

2. Wilson, E. L., "A Digital Computer Program for the Finite Element Analysis of Solids with Nonlinear Material Properties," Technical Memorandum No. 23, Aerojet-General Corporation, Sacramento, July, 1965

3. Hermann, L. R., "A Bending Analysis for Plates," Technical Paper No. 7, SRO, Aerojet-General Corporation, Sacramento, March, 1965

4. Peterson, F. E., "User's Supplement for the Finite Element Analysis of Solids with Nonlinear Material Properties," Aerojet-General Corporation, Sacramento, 7 March 1966

5. Manson, S. S., Thermal Stress and Low-Cycle Fatigue, McGraw-Hill Book Company, 1966

6. Manson, S.S. and Halford, G., "A Method of Estimating High Temperature Low-Cycle Fatigue Behavior of Materials," NASA TMX 522b

7. "Criteria of Section III of the ASME Boiler and Pressure Vessel Code fo Nuclear Vessels," American Society of Mechanical Engineers, New York, 1964

APPENDIX A

STRUCTURAL EVALUATION

Maximum elastic stress (50,000 psi) in the nozzle diaphragm occurs at 16 seconds after startup as a result of the thermal loading condition. The subsequent stress level (10,000 psi) is essentially constant during the remainder of an operational cycle due to the pressure loading condition.

Since the yield strength of S-816 is 38,000 psi, the diaphragm will undergo plastic deformation.

This appendix evaluates the damaging effect of the plastic flow on the basis of low cycle fatigue criteria in terms of A) a conservative value of total strain and B) a more realistic shake-down action.

A. CYCLES-TO-FAILURE, N_f, BASED ON CONSERVATIVE VALUE OF CYCLIC STRAIN RANGE UTILIZING UNIVERSAL SLOPES EQUATION (REF. 5)

WITHOUT REGARD TO THE GEOMETRIC CONFIGURATION AND TEMPERATURE DISTRIBUTION OF THE 2ND STAGE NOZZLE DIAPHRAGM, ASSUME THAT THE MOST SEVERE STRAIN RANGE, $\Delta\epsilon$, OCCURS DUE TO COMPLETE RESTRAINT OF SOME ARBITRARY ELEMENT SUBJECTED TO THE MAXIMUM TEMPERATURE RISE AT 16 SECONDS.

$$\Delta\epsilon_{MAX} = \alpha \Delta T$$

AT 16 SECS

$T_{MAX} = 720°F$

$T_{AMBIENT} = 80°F$

$\alpha = 7.75 \times 10^{-6}$ IN/IN/°F

$$\Delta\epsilon_{MAX} = 7.75 \times 10^{-6} (720 - 80)$$

$$= 4.95 \times 10^{-3} \text{ IN/IN}$$

CYCLIC LIFE, N_f, IS DETERMINED FROM THE UNIVERSAL SLOPES EQUATION (REF. 5)

$$\Delta\epsilon = \frac{3.5\sigma_u}{E} N_f^{-0.12} + D^{0.6} N_f^{-0.6} \quad \text{-----} (1)$$

WHERE

$\Delta\epsilon$ = TOTAL STRAIN RANGE ($\epsilon_{ELASTIC} + \epsilon_{PLASTIC}$), IN/IN

N_f = CYCLES TO FAILURE

σ_u = ULTIMATE TENSILE STRENGTH, PSI

E = MODULUS OF ELASTICITY, PSI

D = DUCTILITY = $LN\left(\frac{100}{100-RA}\right)$ WHERE RA IS PERCENT REDUCTION OF AREA MEASURED FROM TENSILE TEST

FOR S-816 AT 720 °F

$\sigma_u = 118{,}000$ PSI
$E = 28 \times 10^6$ PSI
$RA = 21\%$
$D = LN\left(\frac{100}{100-21}\right) = LN(1.265) = 0.235$

AND EQUATION (1) BECOMES

$$\Delta\epsilon = \frac{3.5(11.8)\times 10^4}{28\times 10^6} N_f^{-0.12} + (0.235)^{0.6} N_f^{-0.6}$$

$$= 1.475\times 10^{-2} N_f^{-0.12} + 0.42 N_f^{-0.6}$$

$$= 1.475\times 10^{-2}\left[N_f^{-0.12} + 28.5 N_f^{-0.6}\right] \quad \text{--------} (2)$$

EQUATION (2) IS PLOTTED IN FIGURE A-1
AND FOR $\Delta\epsilon_{MAX} = 4.95\times 10^{-3}$ IN/IN

N_f = 27,000 CYCLES

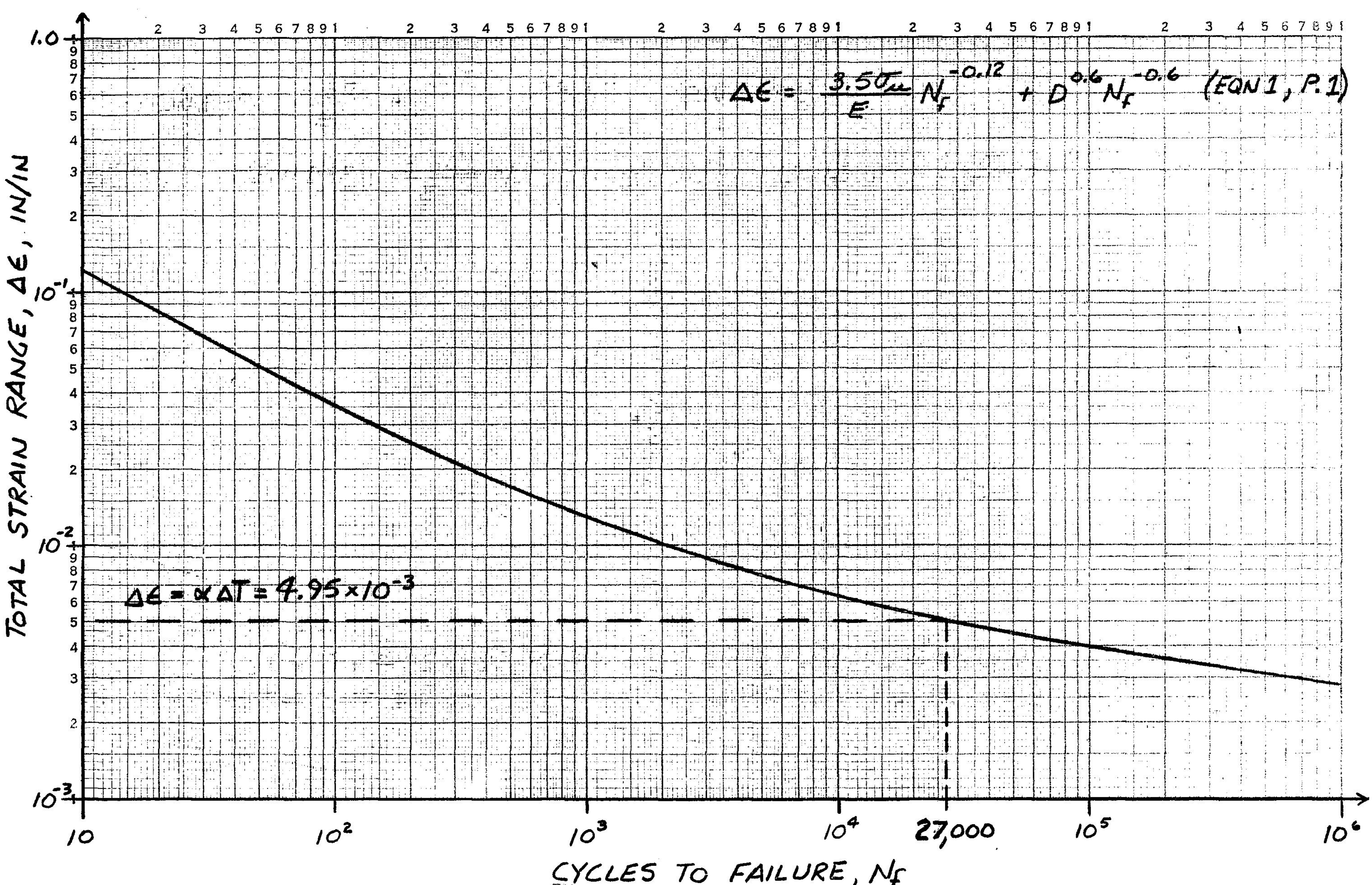

FIGURE A1 - FATIGUE LIFE FOR S-816 AS A FUNCTION OF STRAIN RANGE

ACCORDING TO HIGH TEMPERATURE FATIGUE TEST DATA STUDIED BY MANSON (REF. 6), AN ESTIMATE OF THE LOWER BOUND OF LIFE WAS FOUND TO BE 10% N_f.

USING THIS AS A CRITERIA FOR THE 2ND STAGE NOZZLE DIAPHRAGM THE ESTIMATED LIFE (CYCLES TO FAILURE) IS 2700.

B. PREDICTION OF ACTUAL CYCLIC · BEHAVIOR

SINCE THE TURBINE IS DESIGNED TO OPERATE FOR SEVERAL HUNDRED HOURS PER CYCLE (CYCLE IS DEFINED AS ONE COMPLETE START-UP AND SHUT-DOWN OPERATION) THE MAXIMUM ELASTIC THERMAL STRESS (σ = 50,000 PSI AT T = 16 SECONDS)

CAN BE CONSIDERED AS A THERMAL SHOCK; THE SUBSEQUENT STRESS LEVEL OF 10,000 PSI (DUE TO PRESSURE LOADING) REMAINS CONSTANT THROUGHOUT THE REMAINDER OF THE CYCLE AS SHOWN BELOW IN FIG. A-2.

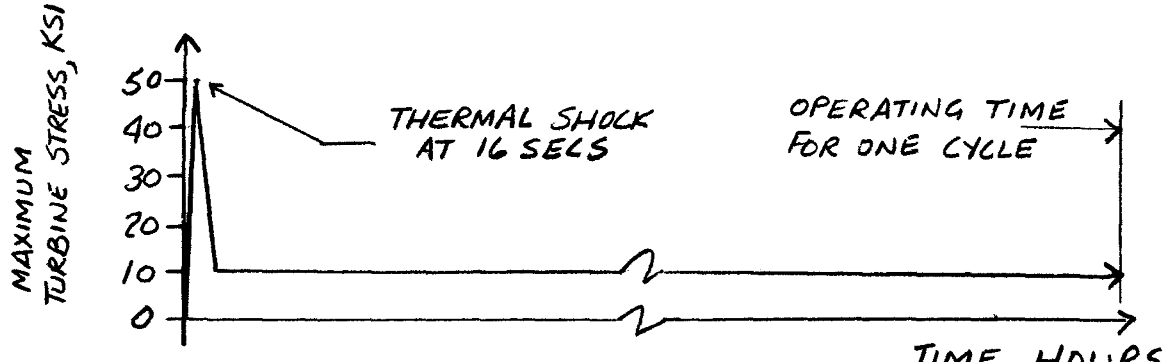

FIGURE A-2 MAXIMUM TURBINE STRESSES DURING ONE OPERATIONAL CYCLE

01-071-002

QUADRILLE WORK SHEET

AEROJET-GENERAL CORPORATION
AZUSA, CALIFORNIA

PAGE A-6 OF ______ PAGES

DATE 27 MAR 1967

SUBJECT 2ND STAGE NOZZLE DIAPHRAGM BY FPB

WORK ORDER 7310·23·100
SNAP·8

1. THERMAL SHOCK

SINCE THE MAXIMUM CALCULATED ELASTIC THERMAL STRESS (50,000 PSI COMPRESSION) IS LESS THAN 2 × YIELD STRESS ($\sigma_{YIELD} = 38{,}000$ PSI) THIS CALCULATED STRESS WILL "SHAKE-DOWN" TO PURELY ELASTIC ACTION AFTER THE FIRST CYCLE. "SHAKE-DOWN" ACTION IS DESCRIBED AS FOLLOWS:

CONSIDER THE OUTER FIBER OF THE SHROUD BEING STRAINED BY THE THERMAL BENDING ACTION OF THE DIAPHRAGM

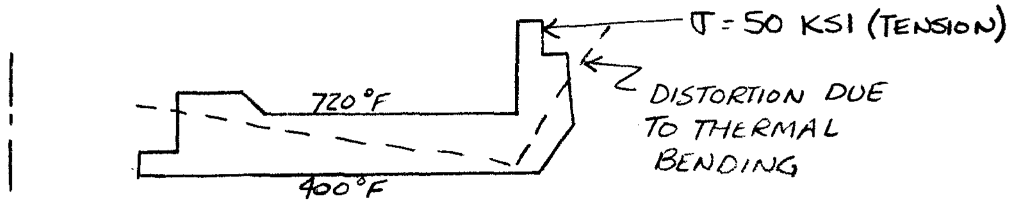

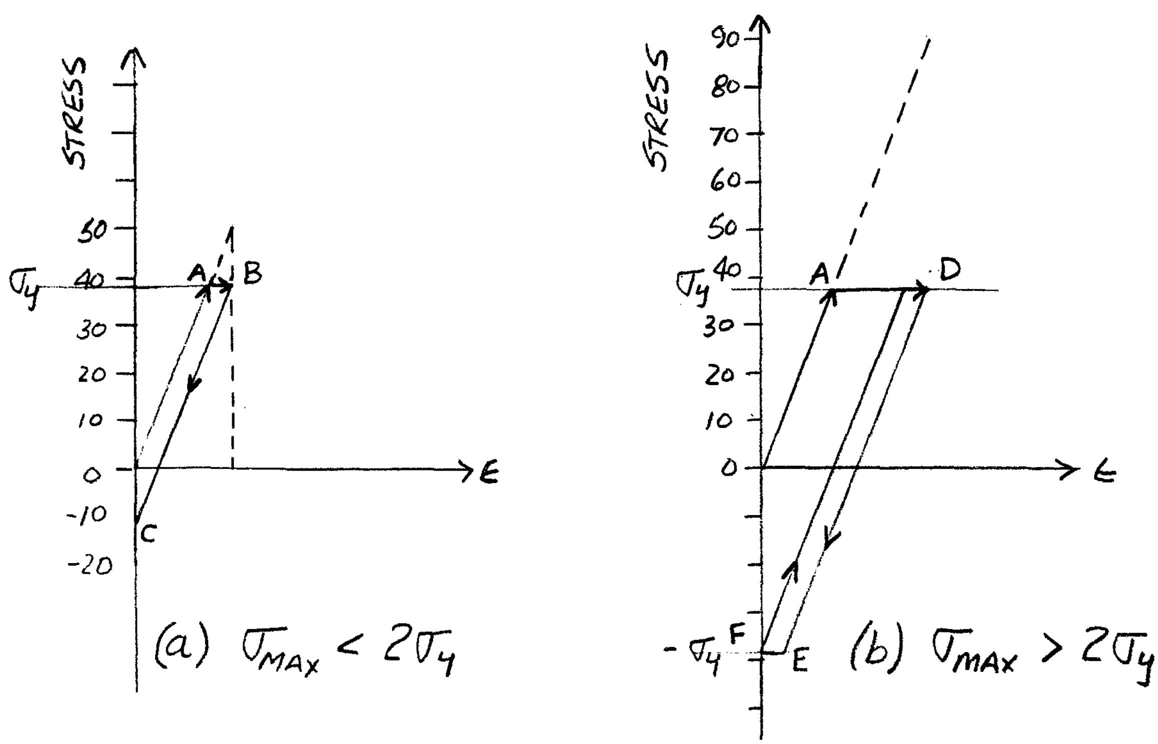

(a) $\sigma_{MAX} < 2\sigma_y$ (b) $\sigma_{MAX} > 2\sigma_y$

FIGURE A-3 STRAIN HISTORY BEYOND YIELD

IF THE MAXIMUM CALCULATED ELASTIC STRESS EXCEEDS THE YIELD OF THE MATERIAL, THIS ELASTIC STRESS WILL OF COURSE NEVER BE ATTAINED. THE STRAIN WILL INCREASE ALONG THE LINE A-B AS SHOWN IN FIGURE A-3(a). AS THE TEMPERATURE GRADIENT THROUGH THE DIAPHRAGM BECOMES LESS SEVERE, THE STRESS AT THE OUTER FIBER OF THE SHROUD CHANGES TO COMPRESSION (B-C); WHEN THE STRUCTURE REACHES EQUILIBRIUM TEMPERATURE, THERE IS A RESIDUAL COMPRESSION STRESS AS SHOWN AT POINT C. ALL SUBSEQUENT CYCLES PRODUCE ELASTIC STRAINING ALONG LINE B-C. THUS THE FIRST CYCLE PRODUCES YIELDING THAT "SHAKES DOWN" TO ELASTIC ACTION.

IF, HOWEVER, THE MAXIMUM ELASTIC STRESS IS GREATER THAN TWICE THE YIELD, AS SHOWN IN FIGURE A-3(b), THE STRAIN PROGRESSES ALONG LINE OADE AND YIELDS IN COMPRESSION TO POINT F. ALL SUBSEQUENT CYCLES PRODUCE PLASTIC STRAIN FROM FD TO EF.

DETAILED EXPLANATION OF THE $2 \times \sigma_{yield}$ CRITERIA AND SUBSEQUENT SHAKE-DOWN IS GIVEN IN REFERENCES (5) AND (7)